US Army Corps of Engineers

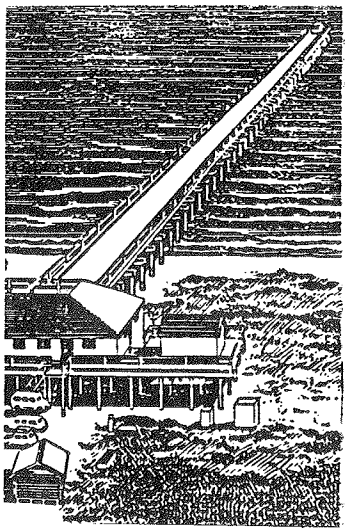

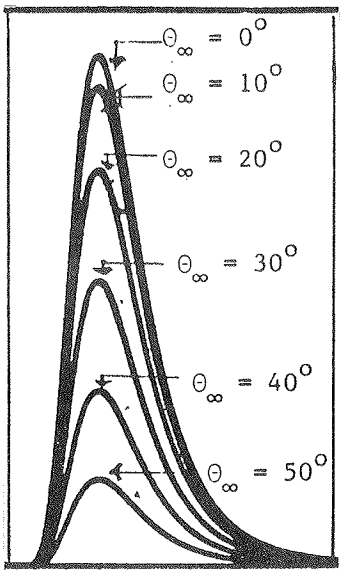

COASTAL ENGINEERING RESEARCH CENTER

MISCELLANEOUS PAPER CERC-89-7

THE EFFECT OF BREAKING WAVES ON THE DIRECTIONAL SPECTRUM OF WAVES IN WATER OF VARIABLE DEPTH IN THE PRESENCE OF CURRENT

by

Chi C. Tung, Yong J. Cho

Department of Civil Engineering
North Carolina State University
Box 7909, Raleigh, North Carolina 27695-7908

US ARMY ENGINEER WATERWAYS EXPERIMENT STATION

June 1989

Final Report

Approved For Public Release; Distribution Unlimited

Prepared for DEPARTMENT OF THE ARMY
US Army Corps of Engineers
Washington, DC 20314-1000

Under Inlet Process Simulation Work Unit 32527

Monitored by Coastal Engineering Research Center
US Army Engineer Waterways Experiment Station
PO Box 631, Vicksburg, Mississippi 39181-0631

Destroy this report when no longer needed. Do not return it to the originator.

The findings in this report are not to be construed as an official Department of the Army position unless so designated by other authorized documents.

The contents of this report are not to be used for advertising, publication, or promotional purposes. Citation of trade names does not constitute an official endorsement or approval of the use of such commercial products.

Unclassified
SECURITY CLASSIFICATION OF THIS PAGE

REPORT DOCUMENTATION PAGE

Form Approved
OMB No. 0704-0188

1a. REPORT SECURITY CLASSIFICATION
Unclassified

1b. RESTRICTIVE MARKINGS

2a. SECURITY CLASSIFICATION AUTHORITY

2b. DECLASSIFICATION / DOWNGRADING SCHEDULE

3. DISTRIBUTION / AVAILABILITY OF REPORT
Approved for public release; distribution unlimited.

4. PERFORMING ORGANIZATION REPORT NUMBER(S)

5. MONITORING ORGANIZATION REPORT NUMBER(S)
Miscellaneous Paper CERC-89-7

6a. NAME OF PERFORMING ORGANIZATION
Department of Civil Engineering

6b. OFFICE SYMBOL (If applicable)

7a. NAME OF MONITORING ORGANIZATION
USAEWES, Coastal Engineering Research Center

6c. ADDRESS (City, State, and ZIP Code)
North Carolina State University
Box 7909, Raleigh, NC 27695-7908

7b. ADDRESS (City, State, and ZIP Code)
PO Box 631
Vicksburg, MS 39181-0631

8a. NAME OF FUNDING / SPONSORING ORGANIZATION
US Army Corps of Engineers

8b. OFFICE SYMBOL (If applicable)

9. PROCUREMENT INSTRUMENT IDENTIFICATION NUMBER

8c. ADDRESS (City, State, and ZIP Code)
Washington, DC 20314-1000

10. SOURCE OF FUNDING NUMBERS

PROGRAM ELEMENT NO.	PROJECT NO.	TASK NO.	WORK UNIT ACCESSION NO.

11. TITLE (Include Security Classification)
The Effect of Breaking Waves on the Directional Spectrum of Waves in Water of Variable Depth in the Presence of Current

12. PERSONAL AUTHOR(S)
Tung, Chi C.; Cho, Yong J.

13a. TYPE OF REPORT
Final report

13b. TIME COVERED
FROM _____ TO _____

14. DATE OF REPORT (Year, Month, Day)
June 1989

15. PAGE COUNT
45

16. SUPPLEMENTARY NOTATION
Available from National Technical Information Service, 5285 Port Royal Road, Springfield, VA 22161.

17. COSATI CODES

FIELD	GROUP	SUB-GROUP

18. SUBJECT TERMS (Continue on reverse if necessary and identify by block number)
See reverse

19. ABSTRACT (Continue on reverse if necessary and identify by block number)

This report details an approximate method for calculating the directional spectrum of waves encountering a current in shallow water. The wave trains in the directional spectrum are assumed to be linear and Gaussian; development of the spectrum requires that the waves also be short crested. The bathymetry is assumed to consist of straight parallel contours. The Miche breaking criterion is imposed to determine the upper limit of wave height and to establish an expression for the breaking wave elevation in terms of the ideal wave's elevation and the second time derivative of elevation. Snell's Law is used for wave refraction. Two examples are given: one for a Wallops directional spectrum encountering a shear current, and one with an upwelling current. Results are presented in graphical form.

20. DISTRIBUTION / AVAILABILITY OF ABSTRACT
☒ UNCLASSIFIED/UNLIMITED ☐ SAME AS RPT. ☐ DTIC USERS

21. ABSTRACT SECURITY CLASSIFICATION
Unclassified

22a. NAME OF RESPONSIBLE INDIVIDUAL

22b. TELEPHONE (Include Area Code)

22c. OFFICE SYMBOL

DD Form 1473, JUN 86 Previous editions are obsolete.

SECURITY CLASSIFICATION OF THIS PAGE
Unclassified

18. SUBJECT TERMS (Continued).

Absolute reference frame, Auto covariance function, Currents, Directional spectra, Miche wave breaking criterion, Plane sloping beach, Probability functions, Relative reference frame, Shear current, Upwelling current.

PREFACE

This report presents results of the development of an approximate method for determining the directional spectrum of breaking waves in finite water depth within a current. The research in this report was authorized by the US Army Corps of Engineers (USACE), under the Harbor Entrances and Coastal Channels Program of Civil Works Research and Development, through "Inlet Process Simulation" Work Unit 32527, at the Coastal Engineering Research Center (CERC) of the US Army Engineer Waterways Experiment Station (WES). Messrs. John H. Lockhart, Jr., John G. Housley, James E. Crews, and Charles W. Hummer of USACE were the Technical Monitors. Dr. Charles L. Vincent of CERC is the Program Manager.

This report was prepared by Drs. Chi C. Tung and Yong J. Cho of North Carolina State University, under IPA No. 87-62-C, Intra-Army Order for Reimbursable Services. The authors appreciate and acknowledge the review and comments provided by personnel of CERC.

The CERC Contract Monitor for this study was Mr. James M. Kaihatu, Coastal Oceanography Branch (CR-O), Research Division (CR), CERC, under direct supervision of Dr. Martin C. Miller, Chief, CR-O, and Mr. H. Lee Butler, Chief, CR; and under general supervision of Mr. Charles C. Calhoun, Jr., and Dr. James R. Houston, Assistant Chief and Chief, CERC, respectively.

Acting Commander and Director of WES was LTC Jack R. Stephens, EN, during report preparation; Technical Director was Dr. Robert W. Whalin.

CONTENTS

	Page
PREFACE	1
PART I: INTRODUCTION	3
PART II: BREAKING WAVE MODEL AND SPECTRUM	4
PART III: WAVE-CURRENT-BOTTOM INTERACTIONS	7
PART IV: NUMERICAL RESULTS	10
PART V: CONCLUSION	13
REFERENCES	14
FIGURES 1-42	
APPENDIX A: NOTATION	A1

THE EFFECT OF WAVE BREAKING ON THE DIRECTIONAL SPECTRUM OF WAVES IN WATER OF VARIABLE DEPTH IN THE PRESENCE OF CURRENT

PART I: INTRODUCTION

1. Waves undergo changes as they propagate from deep to shallow water and/or as they meet an adverse current. The factors that affect these changes include input from local wind, non-linear wave-wave interactions and wave breaking. In this study, only the effect of the last factor is considered.

2. There exists a number of methods to compute changes of wave characteristics under the conditions described above. One analytical method is to use energy balance equation (Phillips, 1980, Huang et al, 1972) but the method does not take into account the effect of wave breaking.

3. In a previous study (Tung and Huang, 1987), a method is developed to study the effect of wave breaking on spectrum of random waves. The waves are assumed to be long-crested, travelling normally toward a straight shoreline over gently varying bottom with straight contours parallel to the shoreline, where they encounter a horizontal current, steady in time and non-uniform in the horizontal space, where flow velocity is parallel to the direction of the waves and is uniformly distributed in depth.

4. The method consists essentially of first assuming that there exists an ideal original wave train at the locale under consideration whose spectrum is obtained using energy balance equation without considering wave breaking. By imposing the Miche wave breaking criterion (Battjes, 1974), an expression for the elevation of breaking waves is established in terms of the elevation of the ideal original waves and its second time derivative which are assumed to be jointly Gaussian. Based on this breaking wave model, a simple but approximate expression for the spectrum of breaking waves is derived in terms of that of the ideal original waves.

5. The purpose of this study is to extend the above method to the case in which the random waves are treated as short-crested whose spectrum has a directional spread. The shoreline is assumed to be straight and the bottom is gently varying with straight contours which are parallel to the shoreline as in the previous study. Two types of steady, non-uniform horizontal currents are considered. The first type is the shear current whose velocity is parallel to the shoreline (see Figure 2). The second type is the upwelling type in which the current velocity is normal to the shoreline. In each case, the current velocity is independent of the alongshore coordinate as well as the vertical coordinate.

6. PART II describes briefly the breaking wave model and gives the expression of the breaking wave spectrum which are respectively established and derived in an earlier report (Tung and Huang, 1987). PART III deals with the mechanics of wave-current interaction for both the shear current and current of the upwelling type without considering wave breaking. In PART IV, numerical results are obtained and presented in graphical form. Some concluding remarks are given in PART V.

PART II. BREAKING WAVE MODEL AND SPECTRUM

7. We assume that waves break whenever the local vertical downward acceleration of the ideal waves reaches a fraction of the gravitational acceleration g* (Phillips, 1980). When this happens, a portion of the mass is detached from the surface, the surface elevation is reduced, and the larger the vertical downward acceleration, the larger the reduction.

8. Referring to Figure 1, let $\zeta(t)$ and $\zeta_b(t)$ represent, respectively, the elevations of the ideal waves and the breaking waves at a fixed point in space where t is time. At points such as A, where $\zeta(t)>0$ and when $\ddot{\zeta}(t)<-Kg$ (see Equation 4 for K), wave breaking occurs and the breaking wave elevation is given by

$$\zeta_b(t) = \zeta(t)\frac{-Kg}{\ddot{\zeta}(t)} \tag{1}$$

Here, and hereafter, overdot denotes differentiation with respect to time.

9. At point B, where $\zeta(t)<0$ and when $\ddot{\zeta}(t)<-Kg$, the breaking wave elevation is given by

$$\zeta_b(t) = \zeta(t)\frac{-\ddot{\zeta}(t)}{Kg} \tag{2}$$

10. Based on the above considerations and noting that no wave breaking takes place when $\ddot{\zeta}(t)>-Kg$, in which case $\zeta(t)$ remains unchanged, $\zeta_b(t)$ may be written as

$$\zeta_b = \zeta\left(-\frac{Kg}{\ddot{\zeta}}\right) H(-\ddot{\zeta}-Kg)H(\zeta)+\zeta\left(\frac{-\ddot{\zeta}}{Kg}\right) H(-\ddot{\zeta}-Kg)H(-\zeta)+\zeta H(\ddot{\zeta}+Kg) \tag{3}$$

where $H(\cdot)$ is the Heaviside unit step function and, for brevity, the argument t in $\zeta_b(t)$, $\zeta(t)$ and $\ddot{\zeta}(t)$ is omitted.

11. For linear waves, the quantity K is shown in the earlier study (Tung and Huang, 1987) to be given by

$$K = 0.44\tanh(\bar{k}_o d) \tag{4}$$

where d is local water depth,

$$\bar{k}_o = \bar{\omega}^2/g \tag{5}$$

---

*For convenience, symbols and abbreviations are listed in the notation (Appendix A).

is characteristic wave number

$$\bar{\omega} = \left[\frac{\int \omega^2 S(\omega)\, d\omega}{\int S(\omega)\, d\omega}\right]^{\frac{1}{2}} \tag{6}$$

is characteristic frequency and $S(\omega)$ is the energy spectrum of the ideal random waves in frequency, ω, space, in deep water.

12. In Equation 3, the breaking wave elevation ζ_b is a nonlinear function of ζ and $\ddot{\zeta}$, the elevation and its second derivative of the original ideal waves which are assumed to the stationary and jointly Gaussian with zero mean values. The determination of the spectrum of ζ_b may therefore be achieved in a straight forward manner (Papoulis, 1965).

13. The spectrum of ζ_b is obtained by first forming its autocorrelation function $R_b(\tau)$ from Equation 3 (where τ is time lag). In doing so, we have neglected the second term in Equation 3 based on the consideration that the probability of occurrence of negative peaks such as point B in Figure 1 is usually small, especially when the spectrum of the waves under consideration is reasonably narrow. In this way, the derivation is much shortened, and our computation shows that the error incurred by ignoring the second term in Equation 3 is indeed imperceptibly small.

14. The resulting autocorrelation function $R_b(\tau)$ is a nonlinear function of the correlation functions $E[\zeta_1\zeta_2]$, $E[\zeta_1\ddot{\zeta}_2]$ and $E[\ddot{\zeta}_1\ddot{\zeta}_2]$ where $E[\cdot]$ denotes the expected value of the quantity enclosed in the brackets and the subscripts 1 and 2 refer to quantities evaluated at time instants $t_1 = t+\tau$ and $t_2 = t$. The autocorrelation $R_b(\tau)$, viewed as a function of these correlation functions, may be expanded by Taylor's series (Borgman, 1965). By retaining only the zeroth and the first order terms of the series and taking the Fourier transform of the resulting approximate autocovariance function , the approximate spectrum of breaking waves is obtained as

$$S_b(\omega) = F(\omega) S(\omega) \tag{7}$$

in which

$$F(\omega) = A_1^2 \left(\frac{\omega^2}{\omega_1^2} - 1\right)^2 \tag{8}$$

is a fourth order polynomial function of ω and may be looked upon as a filter function which accounts for the effect of wave breaking on the spectrum of the ideal waves.

15. The following functions and parameters that appear in Equation 8 are

defined in the following.

$$Z(\eta) = \frac{1}{\sqrt{2\pi}} \exp\left(-\frac{\eta^2}{2}\right) \tag{9}$$

and

$$Q(\xi) = \int_{\xi}^{\infty} Z(\eta)\,d\eta \tag{10}$$

are probability functions (Abramowitz and Stegun, 1968).

$$r = \int S(\omega)\,d\omega \tag{11}$$

$$r^{(2)} = -\int \omega^2 S(\omega)\,d\omega \tag{12}$$

and

$$r^{(4)} = \int \omega^4 S(\omega)\,d\omega \tag{13}$$

are respectively expected values $E[\zeta^2]$, $E[\zeta\ddot{\zeta}]$ and $E[\ddot{\zeta}^2]$,

$$\beta = \frac{Kg}{\sqrt{r^{(4)}}} \tag{14}$$

is a measure of the extent of wave breaking which has been shown to be rather larger than unity (Tung and Huang, 1987) and

$$\varepsilon = 1 - \frac{\left[r^{(2)}\right]^2}{r\ r^{(4)}} \tag{15}$$

which lies between zero and unity is known as the bandwidth parameter of $S(\omega)$ (Cartwright and Longuet-Higgins, 1956).

16. In Equation 8,

$$\omega_1^2 = \left|\frac{A_1}{A_2}\right| \left|\frac{r^{(4)}}{r^{(2)}}\right| \tag{16}$$

$$A_1 = \beta\bar{N} + Q(-\beta) > 0 \tag{17}$$

and

$$A_2 = \beta\bar{N} - \beta Z(\beta)\ Q\left(-\frac{\beta\sqrt{1-\varepsilon^2}}{\varepsilon}\right) - \frac{\beta Q(\beta/\varepsilon)}{\sqrt{2\pi(1-\varepsilon^2)}} + \beta Z(\beta) \tag{18}$$

where

$$\bar{N} = \int_{\beta}^{\infty} \frac{Z(\eta)}{\eta}\ Q\left(-\frac{\sqrt{1-\varepsilon^2}}{\varepsilon}\eta\right) d\eta \tag{19}$$

PART III: WAVE-CURRENT-BOTTOM INTERACTIONS

17. In reference to Figure 2, consider a straight shoreline and assume that the bottom is gently varying with contours parallel to the shore. A random short-crested wave system approaches the shore from deep water and enters a region of current. Two types of horizontal current are considered. The first type is the shear current in which case the horizontal current velocity V(x) is parallel to the shore and independent of the y-coordinate. The second type of current, referred to as the upwelling case, has its velocity U(x) in the x-direction and is also assumed to be independent of the y-coordinate. In each case, the current is steady in time, slowly varying in the horizontal space and independent of the vertical coordinate.

18. The wave system is viewed as a congregate of wave components with distinct frequency ω and angle of approach Θ. For each wave component, the apparent frequency ω, in a stationary frame of reference, is invariant and related to the intrinsic frequency, ω_r, in the frame of reference moving with the current as

$$\omega = \omega_r + \underset{\sim}{U}_H \cdot \underset{\sim}{k} \tag{20}$$

where $\underset{\sim}{U}_H$ is horizontal current velocity vector, $\underset{\sim}{k}$ is wave number vector and

$$\omega_r^2 = gk \tanh(kd) \tag{21}$$

d(x) being the slowly varying local water depth, assumed to be independent of the y - coordinate and k is the magnitude of $\underset{\sim}{k}$. From irrotationality of wave number vector, we have

$$k \sin \Theta = k_\infty \sin\Theta_\infty \tag{22}$$

where the subscript (∞) refers to quantities evaluated in quiescent deep water free of current.

19. Ignoring wave breaking and using the energy balance equation or from conservation of wave action consideration, it was found (Tayfun,et al. 1976) that the wave frequency spectrum $S(\omega,\Theta)$ at the locale under consideration is given by

$$S(\omega,\Theta) = \frac{k(C_G)_\infty\left(1-\frac{\underset{\sim}{U}_H \cdot \underset{\sim}{k}}{\omega}\right)}{k_\infty(C_{gr}+\underset{\sim}{U}_H \cdot \underset{\sim}{k}/k)} \; S_\infty(\omega,\Theta_\infty) \tag{23}$$

where

$$(C_G)_\infty = \frac{\omega}{2k_\infty} \tag{24}$$

is the magnitude of group velocity of deep water waves and

$$C_{gr} = \frac{d\omega_r}{dk} = \frac{\omega_r}{k} n \tag{25}$$

is the magnitude of group velocity of waves in relative frame of reference and

$$n = \frac{1}{2}\left(1 + \frac{2kd}{\sinh(2kd)}\right) \tag{26}$$

for brevity.

20. Thus, for shearing current, $U_H = (0, V(x))$,

$$\omega = \omega_r + Vk \sin\Theta \tag{27}$$

and

$$S(\omega,\Theta) = \frac{k}{2k_\infty} \frac{\omega - Vk\sin\Theta}{c_{gr} + V\sin\Theta} S_\infty(\omega,\Theta_\infty) \tag{28}$$

For the upwelling case, $U_H = (U(x), 0)$,

$$\omega = \omega_r + Uk\cos\Theta \tag{29}$$

and

$$S(\omega,\Theta) = \frac{k}{2k_\infty} \frac{\omega - Uk\cos\Theta}{C_{gr} + U\cos\Theta} S_\infty(\omega,\Theta_\infty) \tag{30}$$

21. To compute the spectrum at a specified locale with given values of water depth d and current velocity U_H, and for a specific wave component of relative frequency ω_r and angle Θ, the corresponding values of wave number k and absolute frequency ω are found from Equations 21 and 20 (or Equations 27, 29) respectively from which the wave number $k_\infty = \omega^2/g$ and angle Θ_∞ (from Equation 22) in deep water are obtained. Finally, $S(\omega,\Theta)$ is computed from Equation 23 (or Equations 28, 30).

22. The wave components are all subject to the breaking limit (Tayfun et al., 1976)

$$C_{gr} + \underset{\sim}{U}_H \cdot \frac{\underset{\sim}{k}}{k} \geq 0 \tag{31}$$

and the kinematic limit

$$\left|\sin\Theta_\infty\right| \leq 1 \tag{32}$$

Those wave components which violate Equation 32 are reflected and the incident wave field is accordingly modified. Such modification, however, is not carried out in this study. Those wave components which violate Equation 31 are cut off and deleted beyond the point under consideration. There also may occur, as is the case in subsequent numerical results, that for specified ω_r, d, U_H and Θ, the energy in deep water, $S_\infty(\omega, \Theta_\infty)$, is very small or non-existent. In that case $S(\omega, \Theta)$ is set equal to zero.

23. To account for the effect of wave breaking, the spectrum $S(\omega,\Theta)$, viewed as a frequency spectrum for specified value of Θ, is first transformed into the frame of reference moving with current. That is

$$\bar{S}(\omega_r,\Theta) = S(\omega,\Theta)\,\frac{d\omega}{d\omega_r} \tag{33}$$

where $d\omega/d\omega_r$ is obtained from Equation 20 (or Equations 27, 29). $\bar{S}(\omega_r,\Theta)$ is then used in place of $S(\omega)$ in Equation 7 from which the breaking wave spectrum in relative frame of reference $\bar{S}_b(\omega_r,\Theta)$ is determined. Spectrum of breaking waves, $S_b(\omega,\Theta)$, in stationary frame of reference, is then calculated by transformation. That is,

$$S_b(\omega,\Theta) = \bar{S}_b(\omega_r,\Theta)\frac{d\omega_r}{d\omega} \tag{34}$$

24. Although the spectra of the breaking waves, in relative and absolute frames of references so obtained as outlined above are, within the confines of the assumptions made, strictly correct, improvements of the results are nevertheless possible by carrying out the computations iteratively. That is, upon obtaining the breaking wave spectrum $\bar{S}_b(\omega_r,\Theta)$ in the relative frame of references, it may be used as the ideal original wave spectrum $S(\omega)$ in Equation 7 from which a revised spectrum $S_b(\omega_r,\Theta)$ results. This process may be repeated until, say, the peak value of $S_b(\omega_r,\Theta)$ converges to within a prescribed limit of tolerance. The breaking wave spectrum $S_b(\omega,\Theta)$ in the stationary frame of reference is then computed according to Equation 34. In this study, the tolerance limit is set at 0.001 m^2/s for all cases considered. The maximum number of cycles of iteration necessary to satisfy this tolerance limit is eight.

25. The iteration process described above, although intuitively appealing and presents no problem in computation, is not without difficulty in theoretical terms since Equation 7 is derived based on the assumption that the ideal waves are a zero mean Gaussian process. However, in the earlier study (Tung and Huang, 1987), it was found that the mean value of ζ_b is rather small and in another study (Tung et al., 1988) the deviation of the probability function of ζ_b from Gaussian is also minimal so that the iterative scheme adopted in this study must be considered acceptable.

PART IV: NUMERICAL RESULTS

26. In order to obtain numerical results, the directional wave spectrum in deep water must be specified. In this study, it is assumed that the directional wave spectrum takes the form

$$S(\omega,\Theta_\infty) = S_\infty(\omega)\Phi(\Theta_\infty) \tag{35}$$

where

$$\Phi(\Theta_\infty) = \frac{8}{3\pi}\cos^4\Theta_\infty \qquad \begin{matrix} |\Theta_\infty| \leq \frac{\pi}{2} \\ |\Theta_\infty| > \frac{\pi}{2} \end{matrix} \tag{36}$$

is the directional energy spreading function. For $S_\infty(\omega)$, there are a great number of frequency spectra (The JONSWAP Spectrum, for example) one can choose from. In this study, we use the wallops spectrum (Huang et al, 1981) which takes the form

$$S_\infty(\omega) = \frac{\alpha g^2}{\omega^m \omega_o^{5-m}} \exp\left[-\frac{m}{4}\left(\frac{\omega_o}{\omega}\right)^4\right] \tag{37}$$

27. The quantity m gives the magnitude of the slope of the frequency spectrum (on log-log scale) in high frequency range and is

$$m = \left|\frac{\log(2\pi^2\S^2)}{\log 2}\right| \tag{38}$$

where

$$\S = \frac{\sqrt{r}}{\lambda_o} \tag{39}$$

is the significant slope of the wave, $\lambda_o = 2\pi/\bar{k}_o$ being the characteristic wave length (see Equation 5). The quantity α is given by

$$\alpha = \frac{m^{(m-1)/4}}{4^{(m-5)/4}} \frac{(2\pi\S)^2}{\Gamma((m-1)/4)} \tag{40}$$

where $\Gamma(\cdot)$ is the gamma function (Abramowitz and Stegun, 1968).

28. The Wallops spectrum is thus seen to depend on two parameters, the significant slope $\S$, which defines m and hence α, and ω_o, which is the frequency corresponding to the peak of the Wallops spectrum. In what follows all numerical results are obtained for values of $\S = 0.015$ and $\omega_o = 0.6$ rad./s.

29. The directional spectrum $S_\infty(\omega,\Theta_\infty)$ in deep water as given by Equation 34 is shown graphically in two ways. In Figure 3, $S_\infty(\omega,\Theta_\infty)$ are given for various values of Θ_∞ as function of ω. Since $S(\omega,\Theta_\infty)$ is symmetrical about $\Theta_\infty = 0$, the spectra are shown only for $0 < \Theta_\infty < \frac{\pi}{2}$. In Figure 4, the contour lines of $S_\infty(\omega,\Theta_\infty)$ are drawn. The ordinates of the contour lines are marked as shown.

30. In the following, we first consider the case in which deep water wave system with $S_\infty(\omega,\Theta_\infty)$ shown in Figures 3 and 4 meets a shear current of V = 2 $^m/_s$ in deep water. Qualitative behavior of wave components on a positive shear current in deep water is shown in Figure 5a and 5b. The ideal wave spectrum $S(\omega,\Theta)$ and the breaking wave spectrum $S_b(\omega,\Theta)$ are given in absolute frame of reference for discrete values of Θ in Figures 6 to 14. The contour lines of $S_b(\omega,\Theta)$ in this case are shown in Figure 15. From Figures 6 to 14, it is seen that most of the wave energy is concentrated near small values of Θ and no wave breaking occurs. For waves with $\Theta = -40^o$, and -30°, the spectra terminate at frequencies 1.205 and 2.208 rad/s respectively. Waves of frequencies beyond these cut-off frequencies originate from regions of $(\omega - \Theta_\infty)$ space where no wave energy exists (see Figure 5b). Waves with $\Theta<0^o$ are subject to limits set by wave breaking but the breaking limits are much larger than the cut-off frequencies shown above. Likewise, waves with $\Theta>0^o$ are subject to kinematic limits and may be reflected. However, these kinematic limits are well beyond frequencies where energy of component waves of any significance exists.

31. We next consider the case in which deep water waves of spectra shown in Figures 3 and 4 encounter an adverse current of the upwelling type with U $=-2^m/_s$ while in deep water. Qualitative behavior of waves on adverse current in deep water is sketched in Figure 16. The ideal wave spectrum $S(\omega,\Theta)$ and the breaking wave spectrum $S_b(\omega,\Theta)$ in absolute frame of reference are given in Figures 17 to 21, for various values of Θ. The contour lines of $S_b(\omega,\Theta)$ are given in Figure 22. Because of symmetry, only spectra and contour lines for $\Theta>0^o$ are shown. As may be expected, wave energy is highest at $\Theta = 0^o$. For waves with $\Theta = 0^o$ and 10°, wave breaking limits the frequencies at $\omega = 1.225$ and 1.244 rad/s respectively where wave energy grows indefinitely. In reality, waves break long before these limits are reached. For waves with $\Theta = 20^o$, 30°, and 40°, waves beyond $\omega = 1.262$, 1.16, and 1.00 respectively do not exist since these originate from regions of $(\omega-\Theta_\infty)$ space where there is no wave (see Figure 16). For $\Theta=0^o$, 10° and 20°, wave breaking reduces the ideal wave spectrum $S(\omega,\Theta)$, but beyond $\Theta = 30^o$, no wave breaking is seen to occur. Other than for the cases of $\Theta = 0^o$ and 10°, the limits set by wave breaking are beyond those cut-off frequencies shown in these Figures. From Figure 22, it is seen that the spectrum $S_b(\omega,\Theta)$ is double peaked.

32. When deep water waves with spectrum given in Figures 3 and 4 propagate toward the shore in still water without current over a gently varying sea bed with straight contours parallel to the straight shoreline, the waves are refracted and bend toward the shore as shown in Figure 16. At water depth d = 10^m, the spectra $S(\omega,\Theta)$ and $S_b(\omega,\Theta)$ are computed and given for discrete values of Θ in Figures 23 to 27 and the contour lines of $S_b(\omega,\Theta)$ are given in Figure 28. Due to symmetry, only cases of $\Theta>0^o$, are given. Most of the wave energy is contained in the neighborhood of $\Theta = 0^o$. For $\Theta = 0^o$, 10° and 20°, wave breaking reduces wave energy, but for waves with $\Theta = 30^o$ and 40°, the effect of wave breaking is vanishingly small. For $\Theta = 10^o$, 20°, 30°, and 40° there exist cut-off frequencies $\omega = 0.197$, 0.370, 0.521, and 0.695 respectively below which no wave exists. These low frequency long waves which are most severely affected by the bottom, originate from regions of $(\omega-\Theta_\infty)$ space where

there is no wave. High frequency short waves are essentially deep water waves unaffected by the bottom.

33. We now consider the case in which the deep water wave system with spectrum shown in Figures 3 and 4 enters a region of shear current of velocity $V = 2^m/_s$ approaching a straight shore over gently varying seabed of straight contours parallel to the beach. At water depth $d = 10^m$, the spectra $S(\omega,\Theta)$ and $S_b(\omega,\Theta)$ in absolute frame of reference are given in Figures 29 to 35 and the contour lines of $S_b(\omega,\Theta)$ are given in Figure 36. Similar to the cases of waves on shear current in deep water and waves approaching the shore without current, wave energy is highest around $\Theta = 0^o$. Wave breaking occurs for waves with $\Theta = -20^o$, -10°, 0°, and 10°, but not for waves with larger values of Θ. Figure 37 gives a sketch of behavior of waves on positive shear current in water of finite depth with parallel contours. Long waves are affected predominantly by the bottom whereas short waves are affected by the current. For waves with $\Theta<0^o$, both short and long waves are bent toward the shore, but for waves with $\Theta>0^o$, short waves bent by the current become increasingly parallel to the shore but refraction by the bottom bends the long waves toward the shore. Thus, in Figures 29 to 35, for both waves with $\Theta<0^o$ and $\Theta>0^o$, there are lower cut-off frequencies of $\omega=0.609$, 0.401, 0.190, 0.197, 0.204, 0.364, and 0.477 rad/s corresponding respectively to cases of $\Theta = -30^o$, -20°, -10°, 0°, 10°, 20°, and 30°. Waves of frequencies below these cut-off frequencies originate from regions of $(\omega-\Theta_\infty)$ space where no wave is present. The short waves travel essentially in deep water on the shear current and behave much the same as those given in section 3 where, for waves with $\Theta = -30^o$, there is an upper cut-off frequency of $\omega = 2.208$ rad/s.

34. The last case considered is that of deep water waves of spectra shown in Figures 3 and 4 encountering a current of the upwelling type with $U = -2^m/_s$ in finite water depth. For waves at water depth $d = 10^m$, the spectra $S(\omega,\Theta)$ and $S_b(\omega,\Theta)$ in absolute frame of reference are given in Figures 38 to 41 and the contour lines of $S_b(\omega,\Theta)$ are given in Figure 42. Because of symmetry, only the cases of $\Theta>0^o$ are given. Energy is concentrated around $\Theta = 0^o$ and wave breaking occurs for waves with $\Theta = 0^o$, 10°, and 20°, but not for waves with $\Theta = 30^o$ much the same as in the case of deep water waves meeting an upwelling current in deep water. Both short and long waves are bent toward the shore with the short waves affected by the current and the long waves by the sea bottom. Thus, for the short waves, there are upper cut-off frequencies, as limited by wave breaking of $\omega = 1.225$ and 1.244 rad/s corresponding to waves with $\Theta = 0^o$ and 10° respectively. For waves with $\Theta = 20^o$ and 30°, the upper cut-off frequencies are respectively $\omega = 1.262$ and 1.15 rad/s, as in the case of waves encountering an upwelling current in deep water. For the long waves, the lower cut-off frequencies are $\omega = 0.234$, 0.450 and 0.739 rad/s corresponding respectively to the cases of $\Theta = 10^o$, 20° and 30°. Waves of frequencies below these values originate from regions of $(\omega-\Theta_\infty)$ space where no wave exists.

PART V: CONCLUSION

35. In an earlier report (Tung and Huang, 1987) we introduced a method by means of which the effect of wave breaking or wave spectrum can be incorporated. The method was applied to the case in which a uni-directional deep water wave system propagates toward the shore over gently varying sea bed of straight parallel contours encountering an adverse current. In this report, the method is extended to the case in which the deep water wave system represented by a directional spectrum propagating over a sea bed having the same characteristics meeting current of either the shearing type parallel to the shore or of the upwelling type perpendicular to the shore.

36. The method of incorporating wave breaking is approximate, but easy to apply. The solution to the wave-current interaction problem (without considering wave breaking) is for the specific case where the sea bed has parallel contours. The results so obtained are therefore restricted in application. The method of dealing with wave breaking can be improved, but such refinement is not considered necessary at this stage of development. The restriction imposed by the idealization of the sea bed can be relaxed by adopting a fully numerical treatment of the wave-current interaction problem (without considering wave breaking).

37. The results of this study must be checked against those of other analytical methods and experimental data, both from the field and laboratory.

REFERENCES

Abramowitz, M., and Stegun, I. A. 1968, Handbook of Mathematical Functions, Dover Publications, Inc., New York, N.Y., pp 228-936.

Battjes, J. A. 1974. "Computation of Set-up, Long Shore Currents, Run-up and Overtopping due to Wind-generated Waves," Communications on Hydraulics No. 74-2, Department of Civil Engineering, Delft University of Technology, Delft, The Netherlands.

Borgman, L. E. 1965. "A Statistical Theory for Hydrodynamic Forces on Objects," Technical Report HEL-9-6, Hydraulics Engineering Laboratory, University of California, Berkeley, Calif.

Cartwright, D. E., and Longuet-Higgins, M. S. 1956. "The Statistical Distribution of the Maxima of a Random Function," "Proceedings of the Royal Society of London, Ser A, Vol 237, pp 212-232.

Huang, N.E., Chen, P.T., Tung, C.C., Smith, J. 1972. "Interactions Between Steady Non-uniform Currents and Gravity Waves with Applications for Current Measurements", Journal of Physical Oceanography, Vol. 2, No. 4, pp 420-431.

Huang, N. E., Long, S. R., Tung, C. C., Yuan, Y., and Bliven, L. F. 1981. "A Unified Two-parameter Wave Spectral Model for a General Sea State, Journal of Fluid Mechanics, Vol 112, pp 203-224.

Papoulis, A. 1965. Probability, Random Variables, and Stochastic Processes, McGraw-Hill Book Co., Inc., New York, NY., pp 206-221, 239-258.

Phillips, O. M. 1980. The Dynamics of the Upper Ocean, Cambridge University Press New York, N.Y., p 142.

Tayfun, M. A., Dalrymple, R. A. and Yang, C. Y. 1976. "Random Wave-Current Interactions in Water of Varying Depth," Ocean Engineering, Vol. 3, No. 6, pp 403-420.

Tung, C. C., and Huang, N. E. 1987. "Breaking Wave Spectrum in Water of Finite Depth in the Presence of Currents," Technical Report CERC-87-19, Department of the Army, US Army Corps of Engineers, Washington, DC.

Tung, C. C., Huang, N. E., Yuan, Y. and Long, S. R. 1988. "Probability Function of Breaking Limited Surface Elevation," Journal of Geophysical Research, to appear.

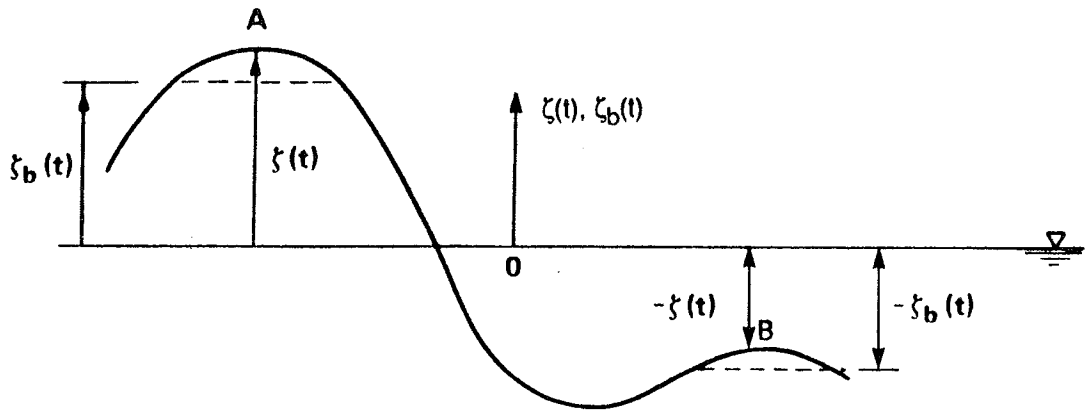

Figure 1. Wave profile

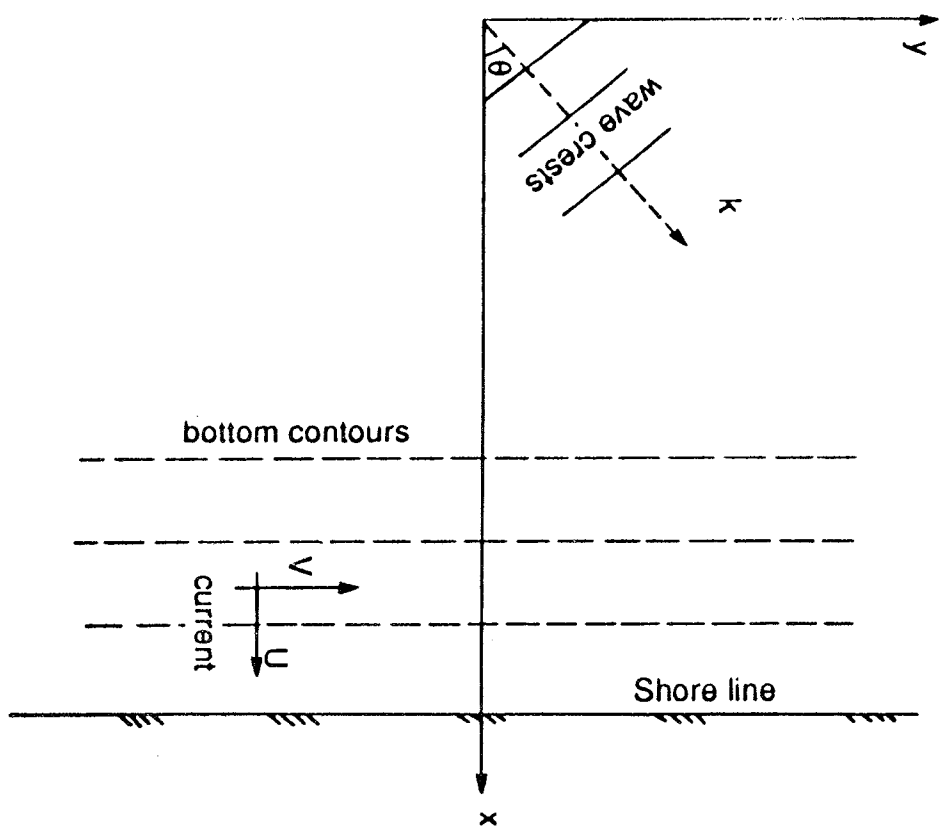

Figure 2. Definition sketch of wave, current and bottom contour

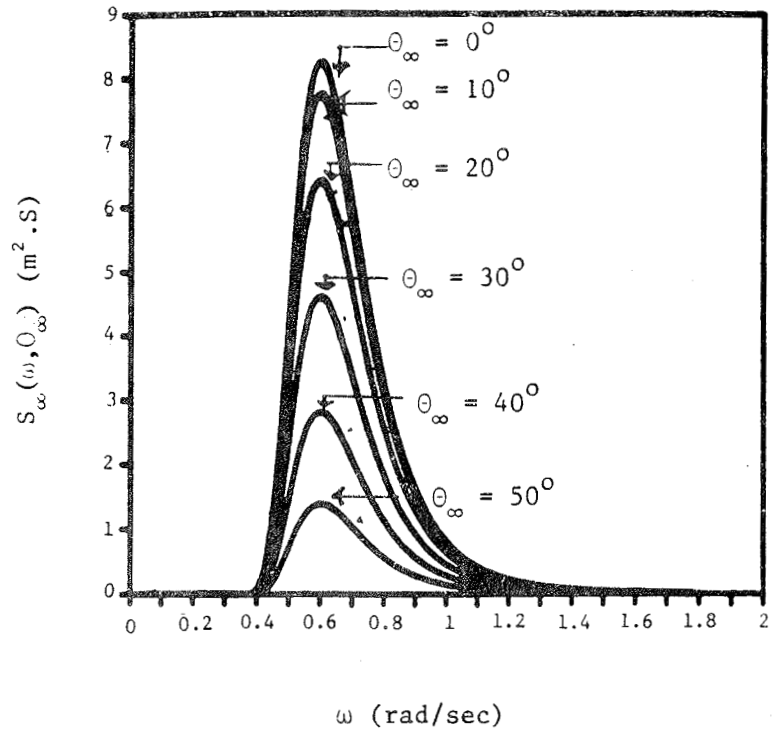

Figure 3. Spectra $S_\infty(\omega,\Theta_\infty)$ of deep water waves under zero current condition, for $\Theta_\infty = 0°$, 10°, 20°, 30°, 40°, and 50°, and for $\S = 0.015$ and $\omega_o = 0.6$ rad/sec

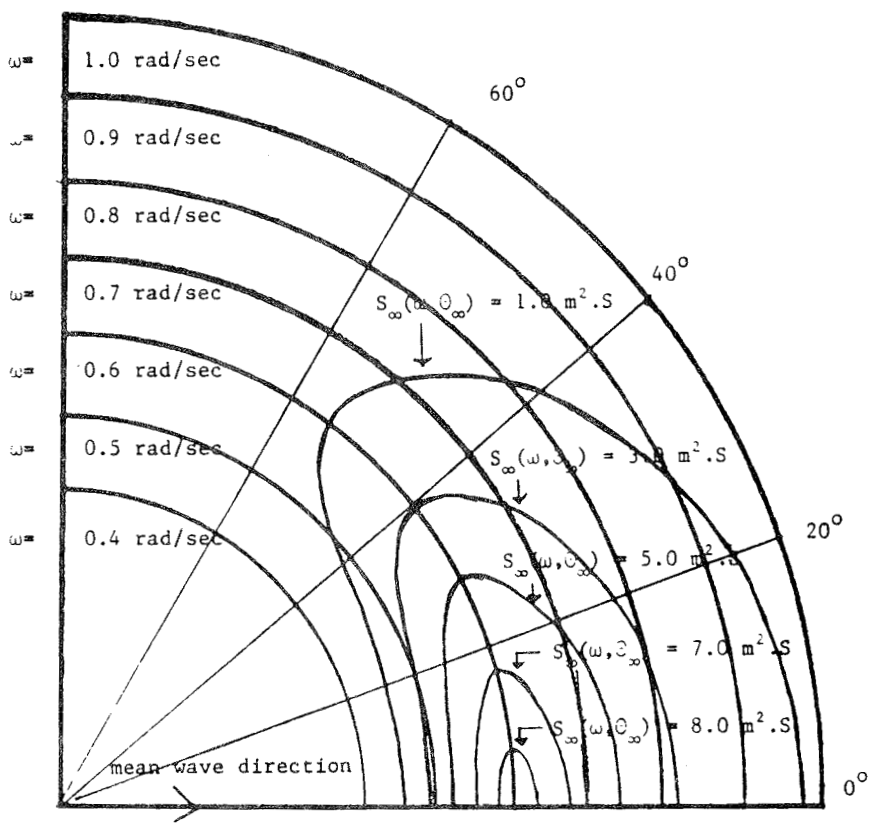

Figure 4. Contour lines of $S_\infty(\omega,\Theta)$ of deep water waves under zero current condition, for $\S = 0.015$ and $\omega_o = 0.6$ rad/sec

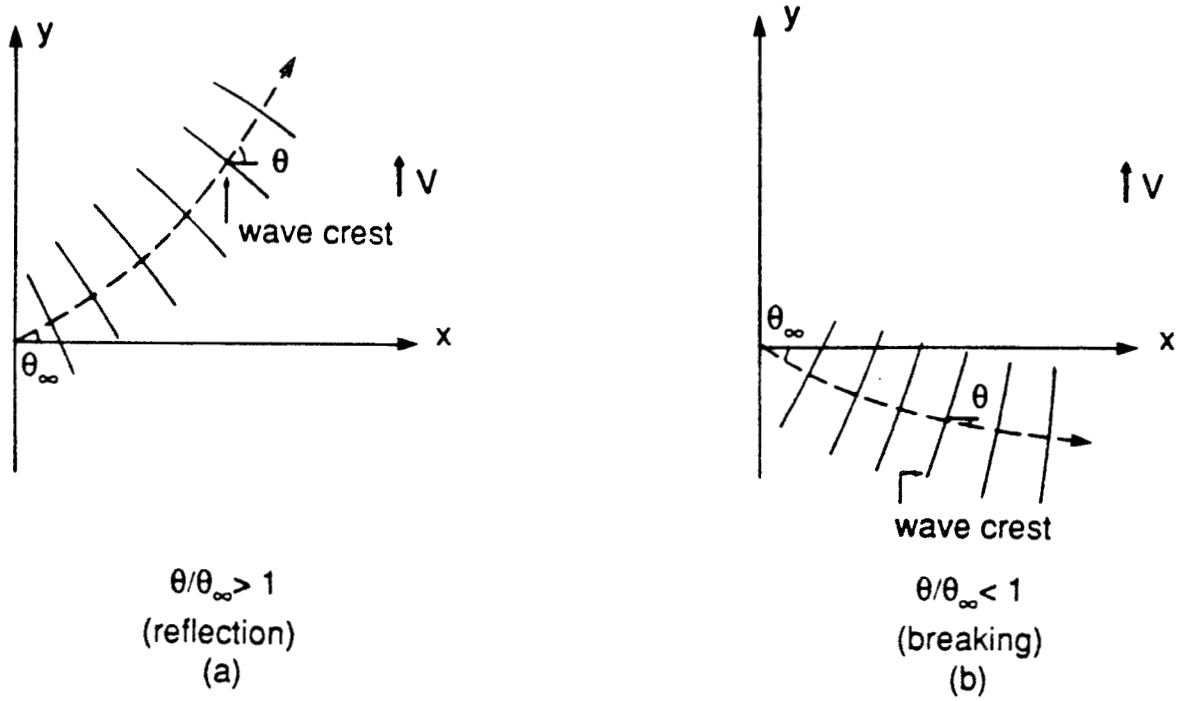

Figure 5. Qualitative behavior of deep water waves on positive shear current

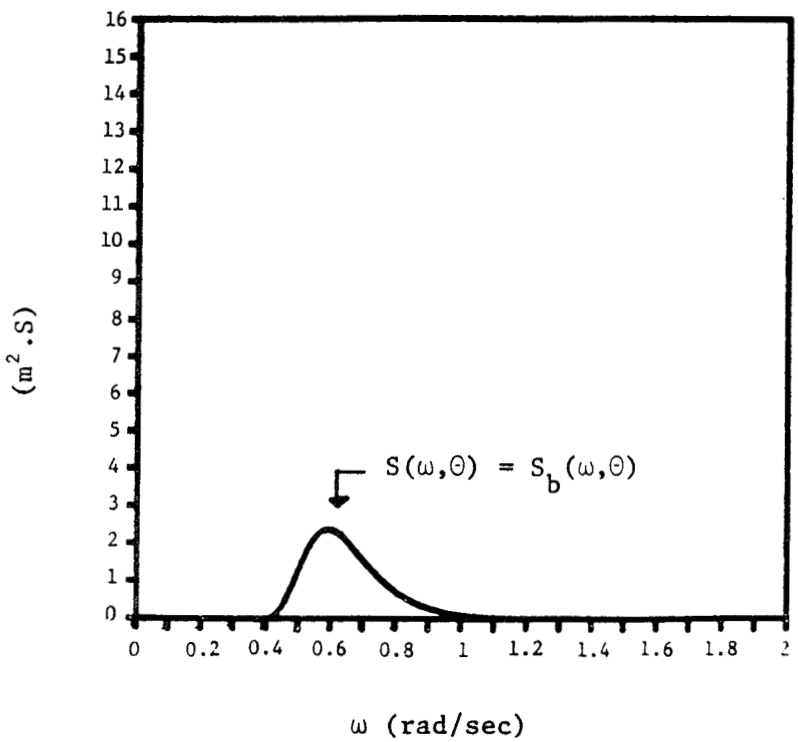

Figure 6. Spectra $S(\omega,\Theta)$ and $S_b(\omega,\Theta)$ of deep water waves on current with $V = 2^m/_s$, for $\Theta = -40°$, and for $\S = 0.015$ and $\omega_o = 0.6$ rad/sec

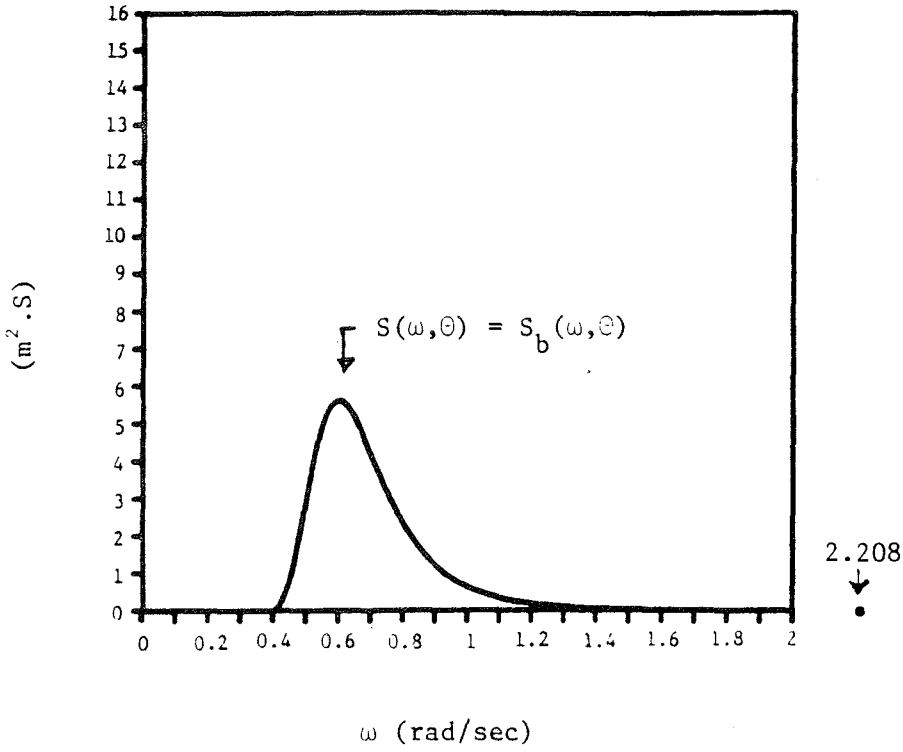

Figure 7. Spectra $S(\omega,\Theta)$ and $S_b(\omega,\Theta)$ of deep water waves on current with $V = 2^m/_s$, for $\Theta = -30°$, and for $\S = 0.015$ and $\omega_o = 0.6$ rad/sec

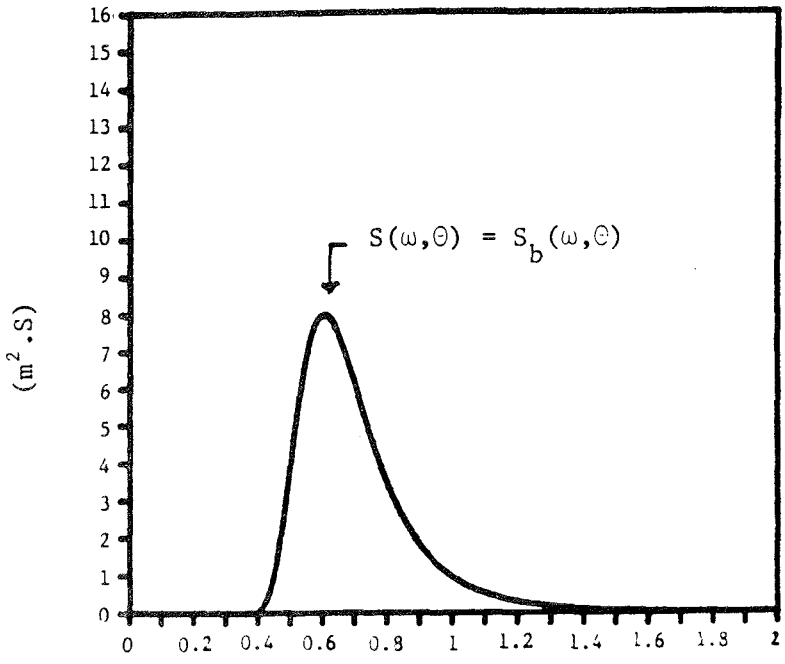

Figure 8. Spectra $S(\omega,\Theta)$ and $S_b(\omega,\Theta)$ of deep water waves on current with $V = 2^m/_s$, for $\Theta = -20°$, and for $\S = 0.015$ and $\omega_o = 0.6$ rad/sec

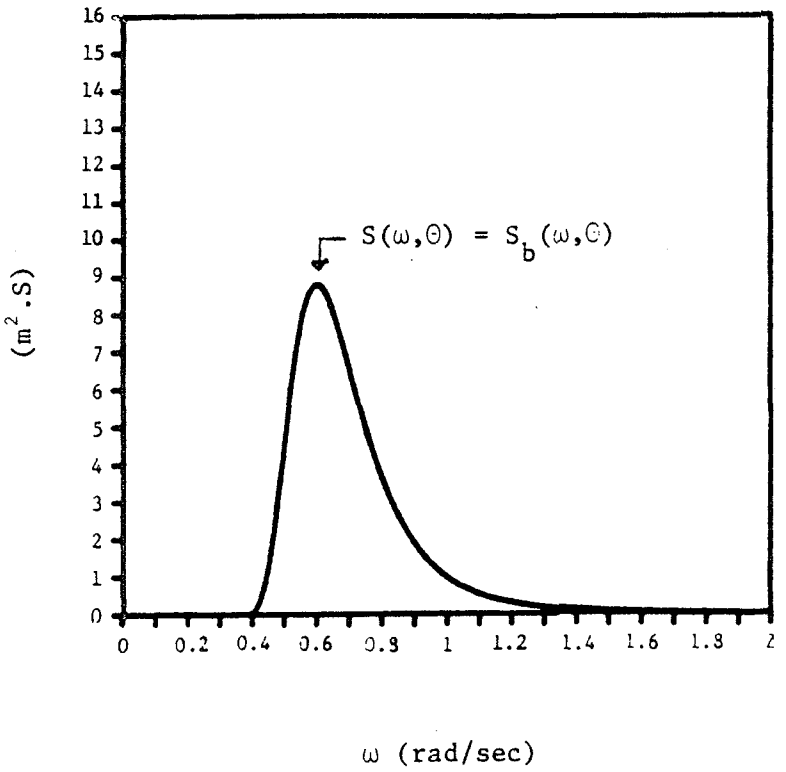

Figure 9. Spectra $S(\omega,\Theta)$ and $S_b(\omega,\Theta)$ of deep water waves on current with $V = 2^m/_s$, for $\Theta = -10°$, and for $\S = 0.015$ and $\omega_o = 0.6$ rad/sec

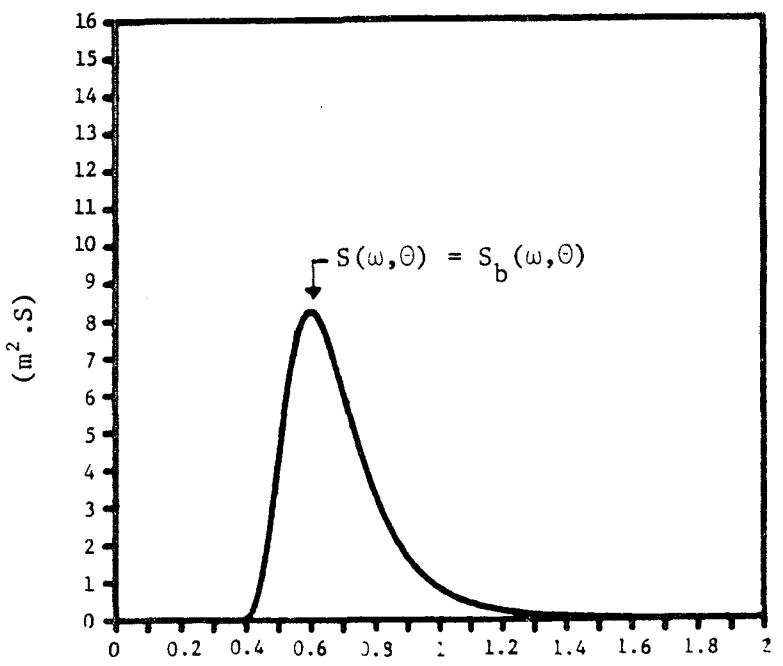

Figure 10. Spectra $S(\omega,\Theta)$ and $S_b(\omega,\Theta)$ of deep water waves on current with $V = 2^m/_s$, for $\Theta = 0°$, and for $\S = 0.015$ and $\omega_o = 0.6$ rad/sec

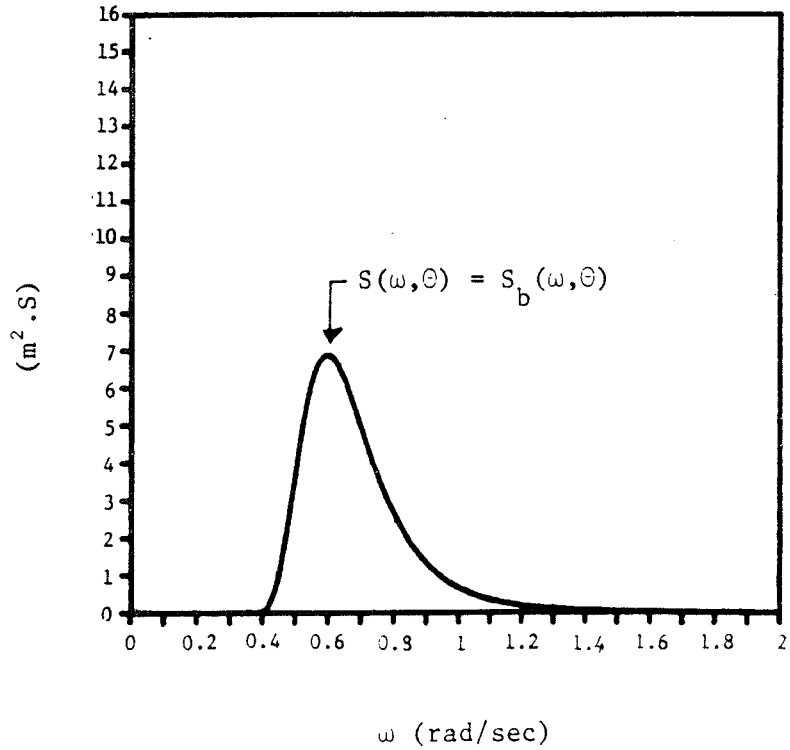

Figure 11. Spectra $S(\omega,\Theta)$ and $S_b(\omega,\Theta)$ of deep water waves on current with $V = 2^m/_s$, for $\Theta = 10°$, and for $\S = 0.015$ and $\omega_o = 0.6$ rad/sec

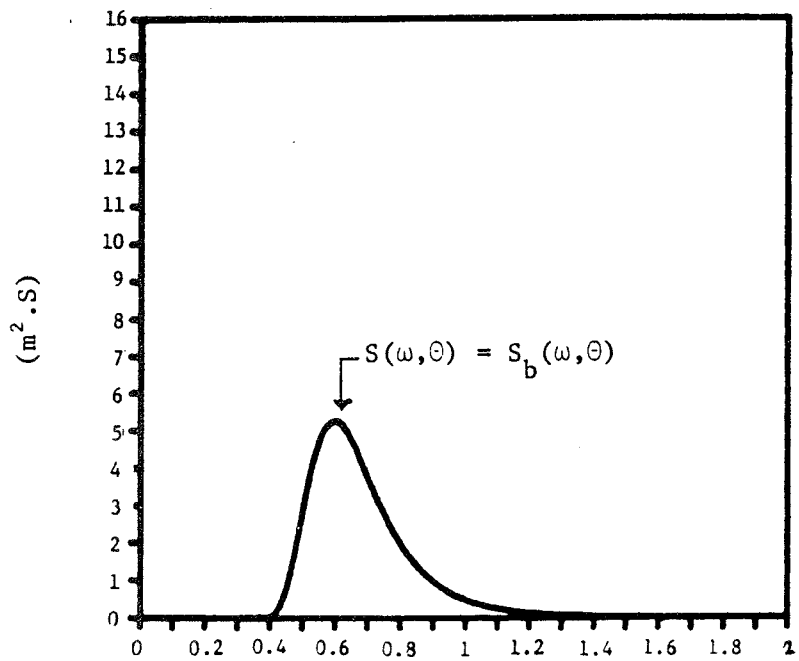

Figure 12. Spectra $S(\omega,\Theta)$ and $S_b(\omega,\Theta)$ of deep water waves on current with $V = 2^m/_s$, for $\Theta = 20°$, and for $\S = 0.015$ and $\omega_o = 0.6$ rad/sec

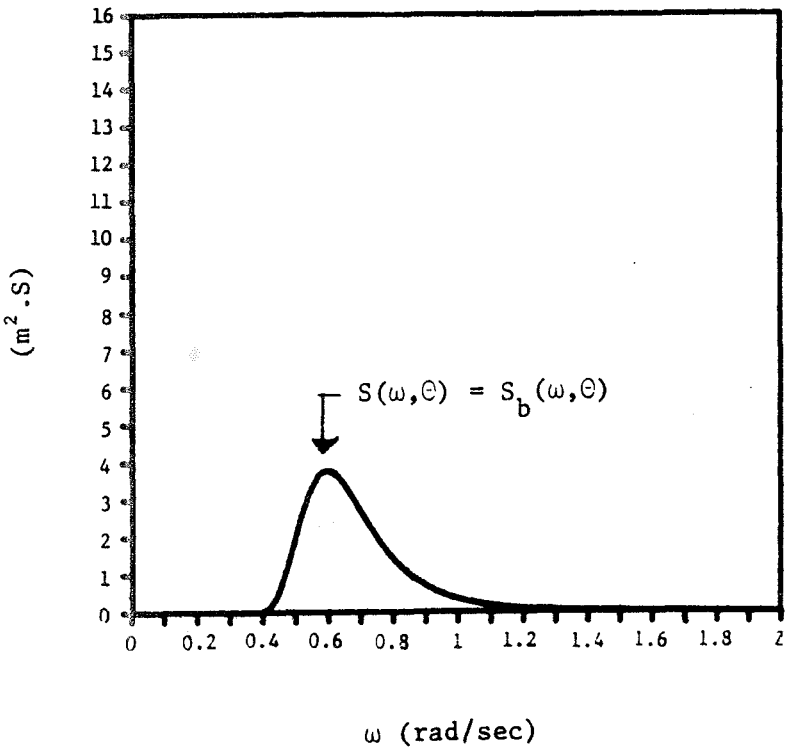

Figure 13. Spectra $S(\omega,\Theta)$ and $S_b(\omega,\Theta)$ of deep water waves on current with $V = 2^m/_s$, for $\Theta = 30°$, and for $\S = 0.015$ and $\omega_o = 0.6$ rad/sec

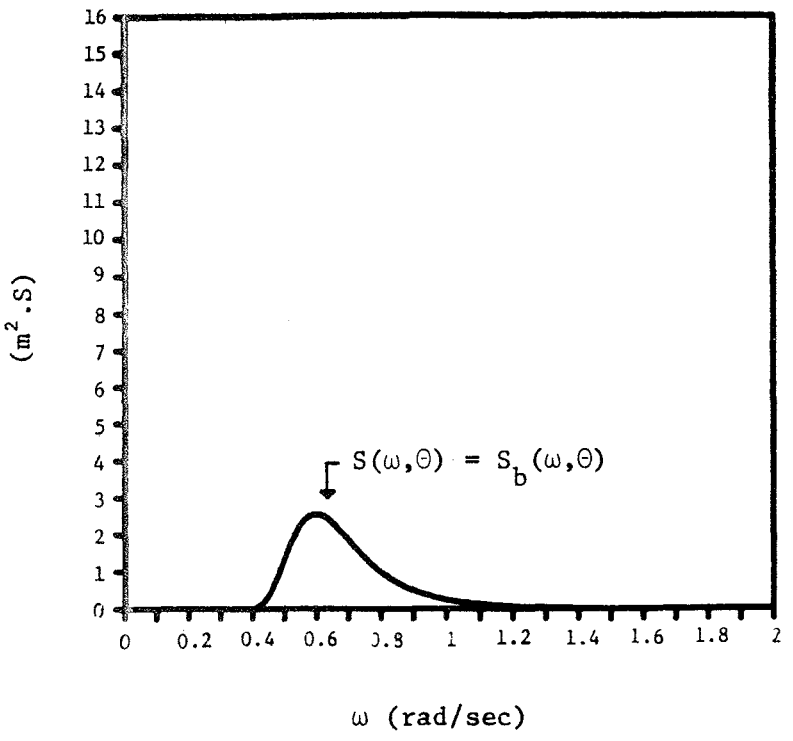

Figure 14. Spectra $S(\omega,\Theta)$ and $S_b(\omega,\Theta)$ of deep water waves on current with $V = 2^m/_s$, for $\Theta = 40°$, and for $\S = 0.015$ and $\omega_o = 0.6$ rad/sec

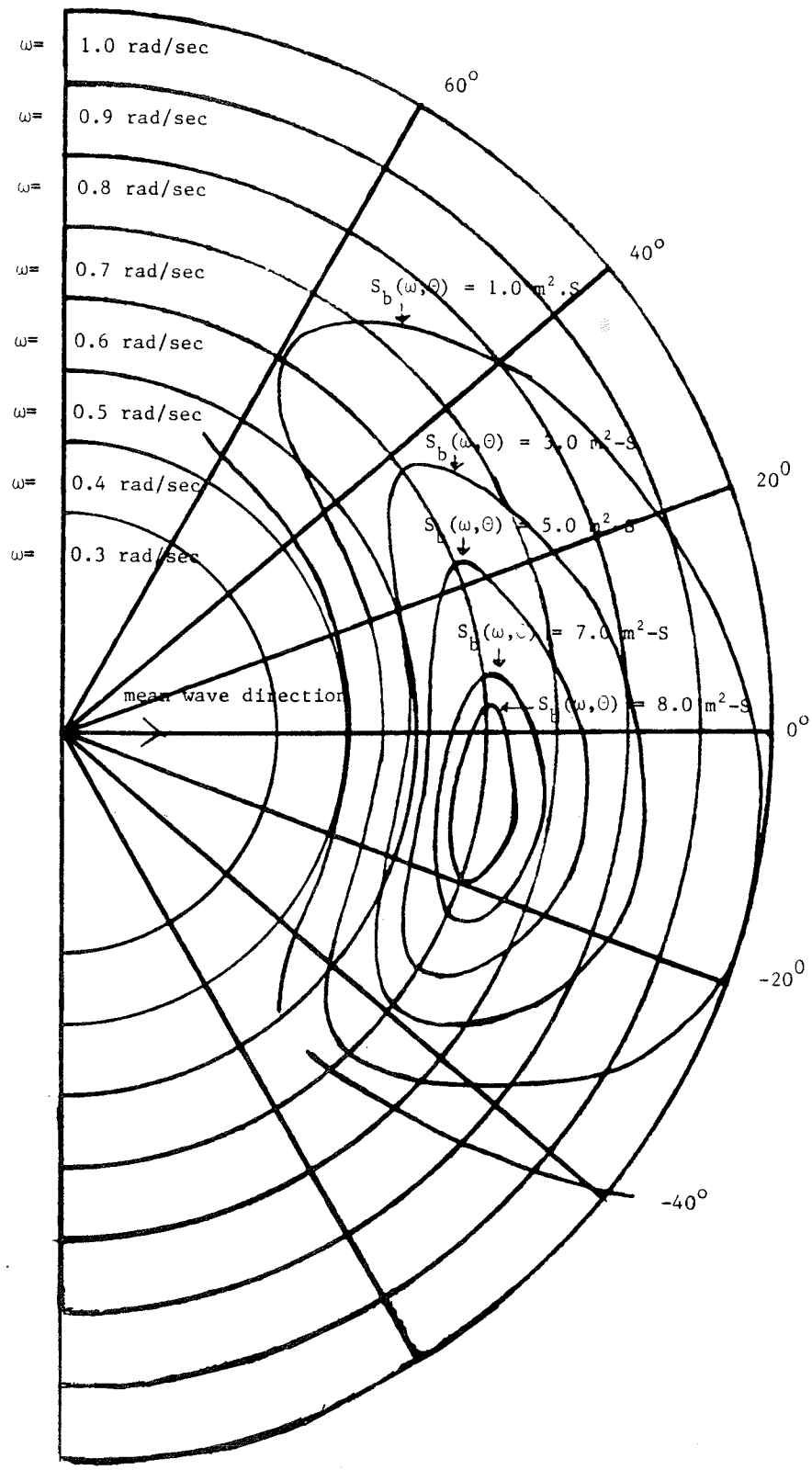

Figure 15. Contour lines of $S_b(\omega,\Theta)$ of deep water waves on current with $V = 2^m/_s$, for $\S = 0.015$ and $\omega_o = 0.6$ rad/sec

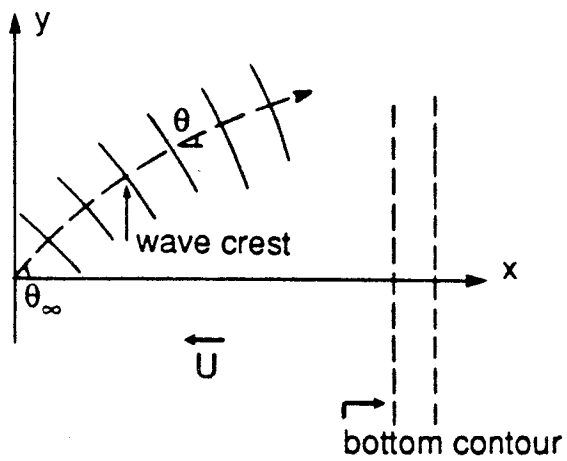

Figure 16. Qualitative behavior of deep water waves on adverse current of upwelling type and of waves over bottom of parallel contours

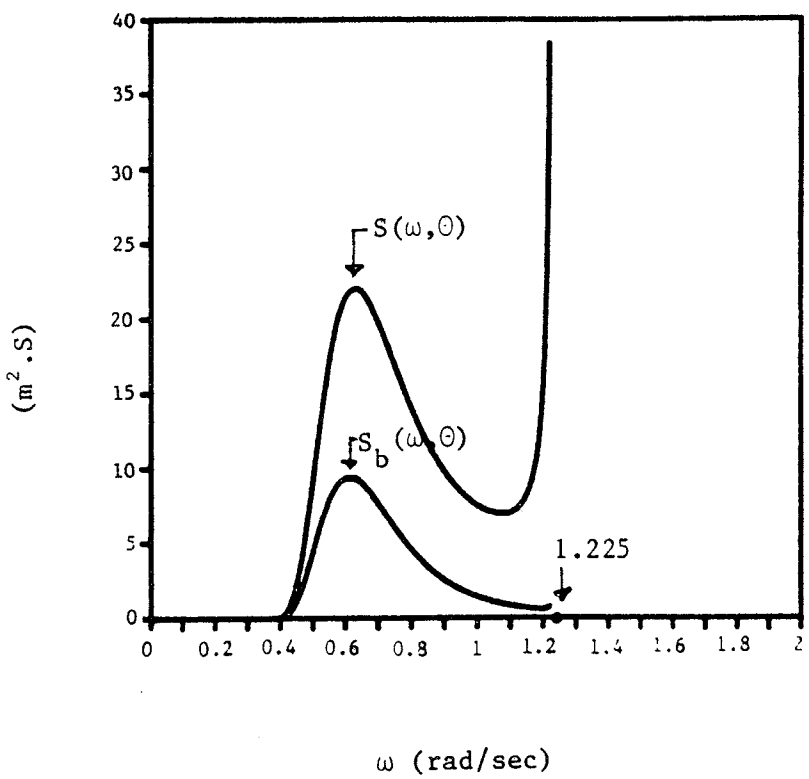

Figure 17. Spectra $S(\omega,\Theta)$ and $S_b(\omega,\Theta)$ of deep water waves on current with $U = -2^m/_s$, for $\Theta = 0°$, and for $\S = 0.015$ and $\omega_o = 0.6$ rad/sec

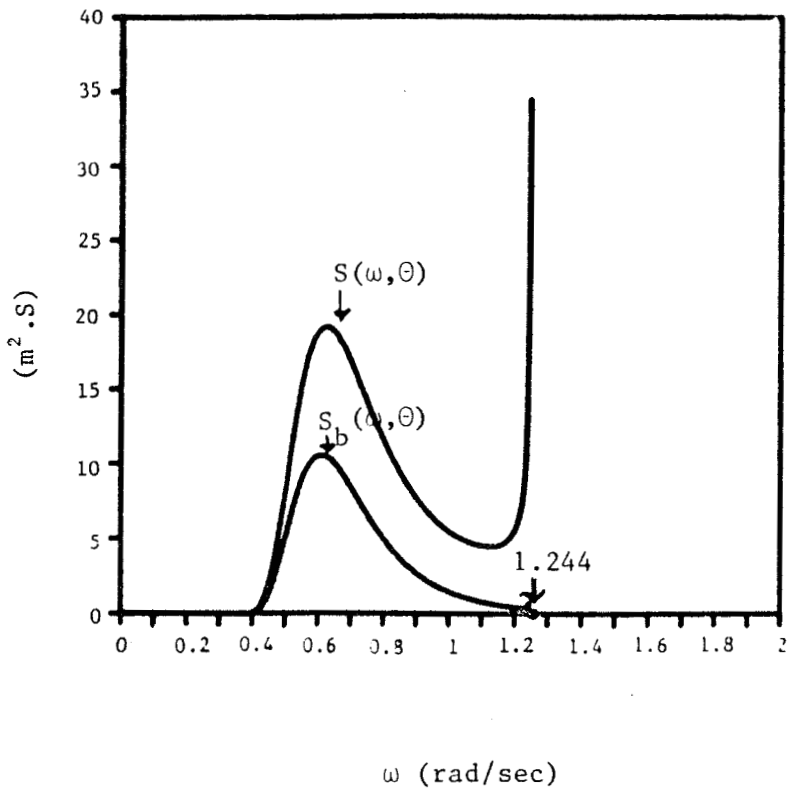

Figure 18. Spectra $S(\omega,\Theta)$ and $S_b(\omega,\Theta)$ of deep water waves on current with $U = -2^m/_s$, for $\Theta = 10°$, and for $\S = 0.015$ and $\omega_o = 0.6$ rad/sec

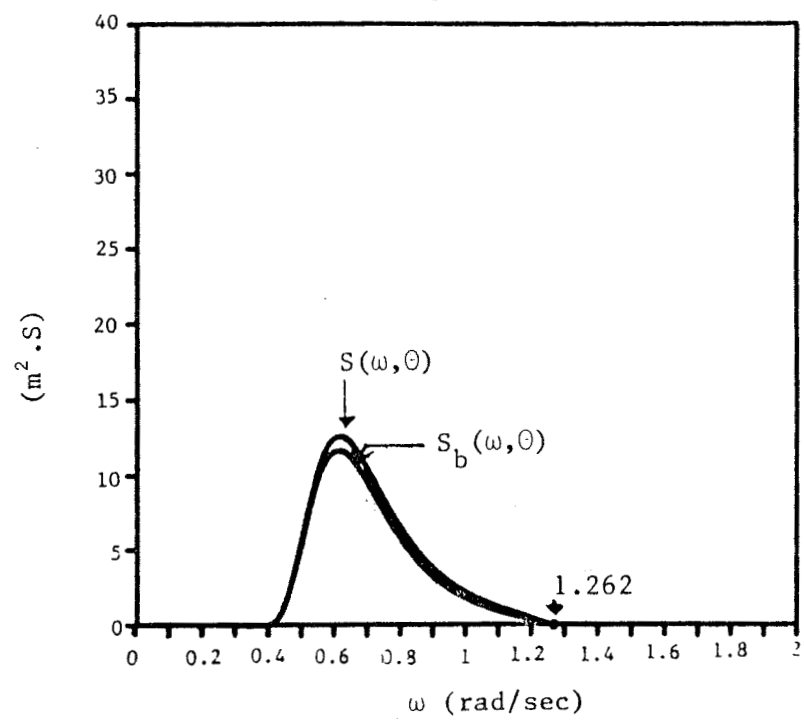

Figure 19. Spectra $S(\omega,\Theta)$ and $S_b(\omega,\Theta)$ of deep water waves on current with $U = -2^m/_s$, for $\Theta = 20°$, and for $\S = 0.015$ and $\omega_o = 0.6$ rad/sec

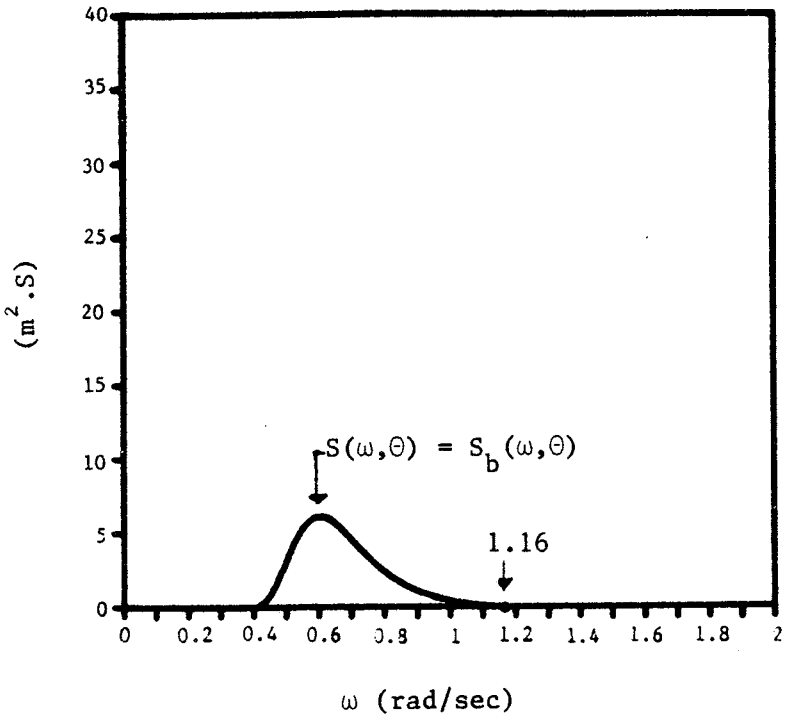

Figure 20. Spectra $S(\omega,\Theta)$ and $S_b(\omega,\Theta)$ of deep water waves on current with $U = -2^m/_s$, for $\Theta = 30°$, and for $\S = 0.015$ and $\omega_o = 0.6$ rad/sec

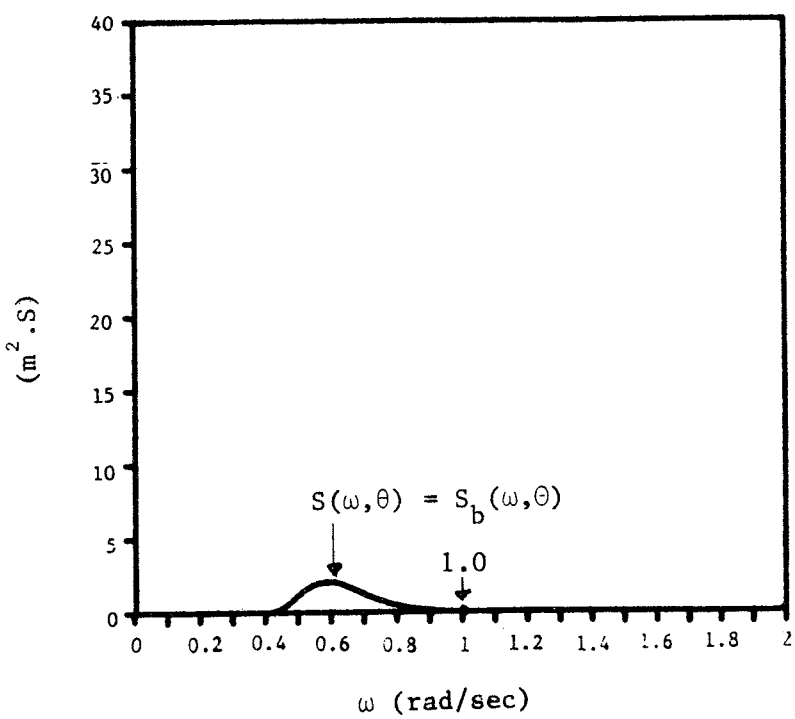

Figure 21. Spectra $S(\omega,\Theta)$ and $S_b(\omega,\Theta)$ of deep water waves on current with $U = -2^m/_s$, for $\Theta = 40°$, and for $\S = 0.015$ and $\omega_o = 0.6$ rad/sec

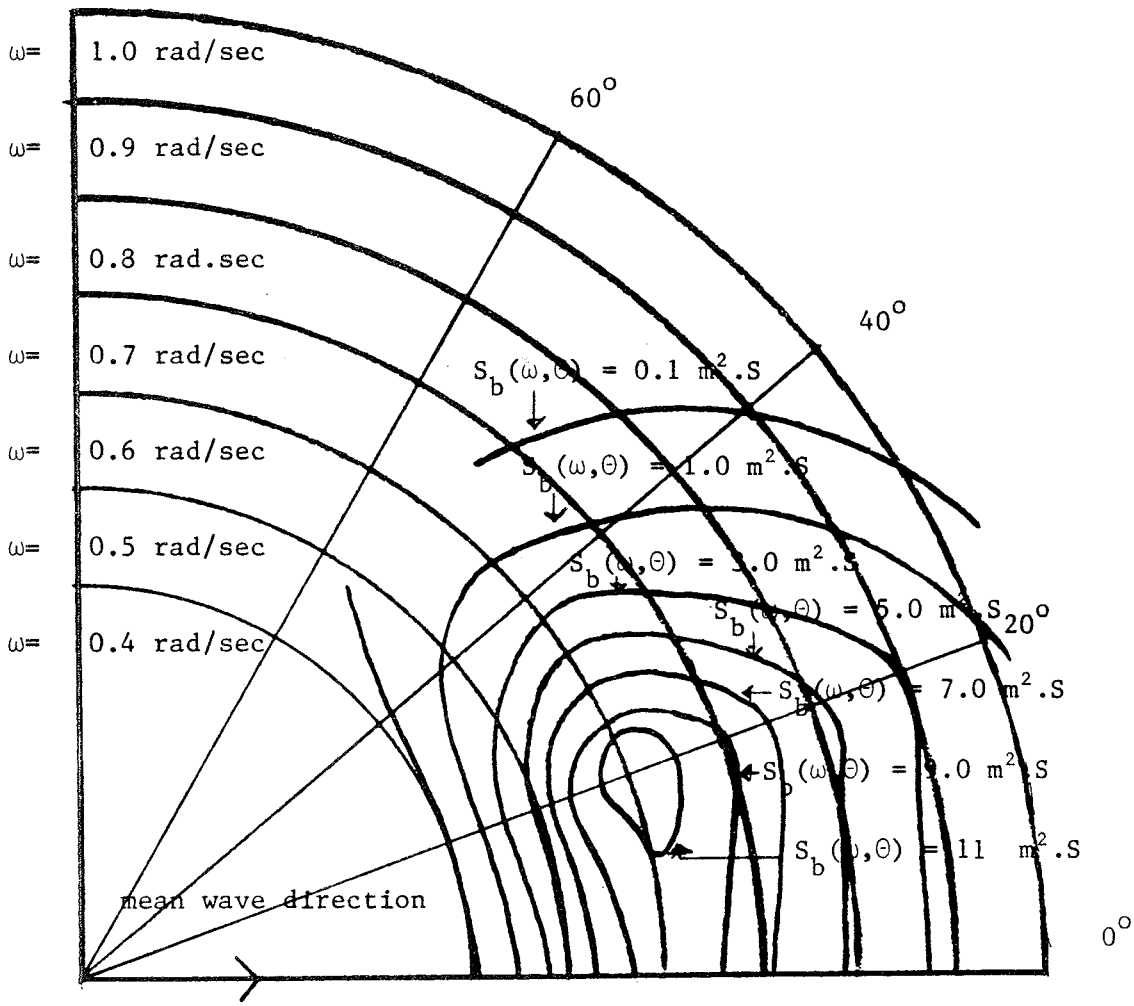

Figure 22. Contour lines of $S_b(\omega\ \Theta)$ of deep water waves on current with $U = -2^m/_s$, for § = 0.015 and ω_o = 0.6 rad/sec

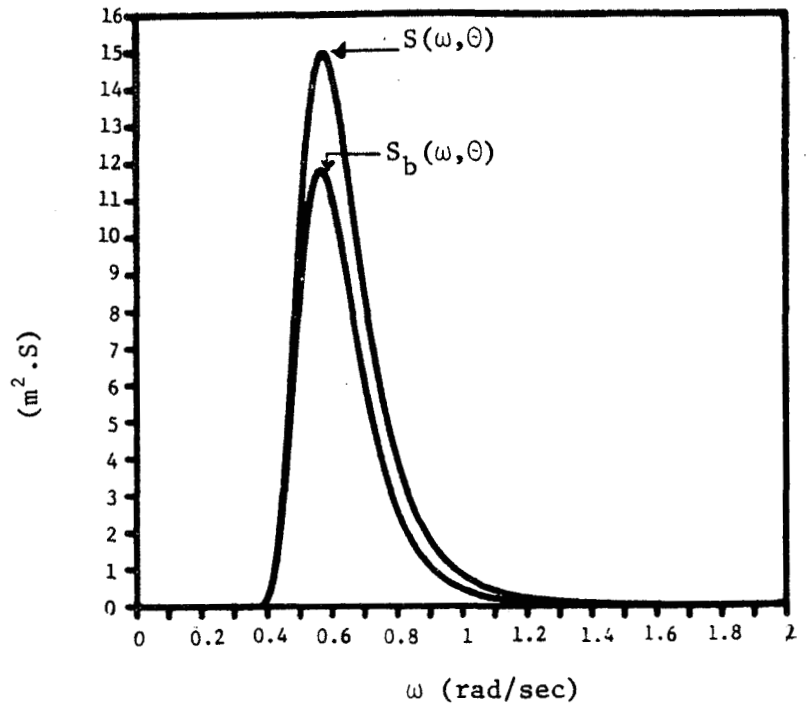

Figure 23. Spectra $S(\omega,\Theta)$ and $S_b(\omega,\Theta)$ of waves at water depth $d = 10^m$ under zero current condition, for $\Theta = 0°$, and $\S = 0.015$ and $\omega_o = 0.6$ rad/sec

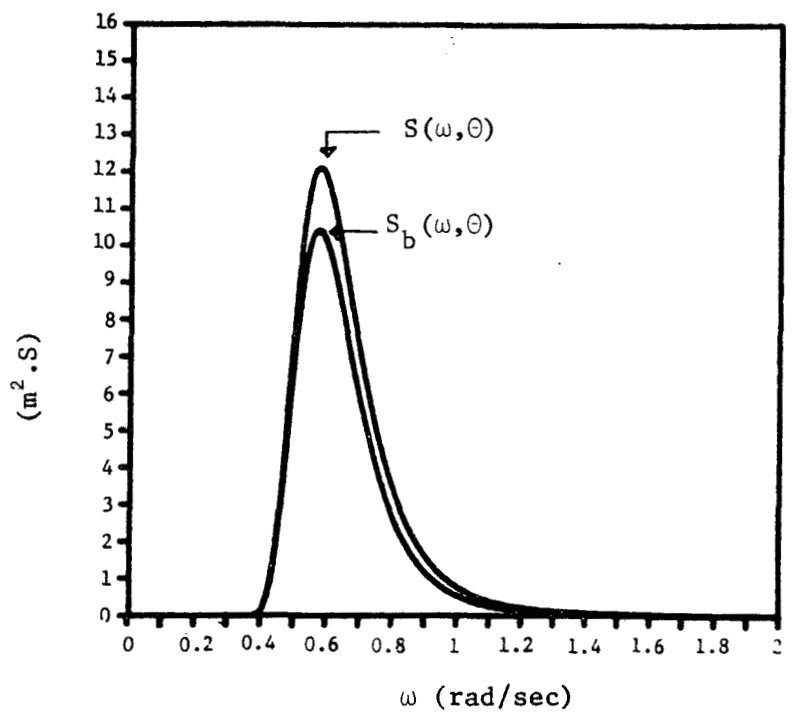

Figure 24. Spectra $S(\omega,\Theta)$ and $S_b(\omega,\Theta)$ of waves at water depth $d = 10^m$ under zero current condition, for $\Theta = 10°$, and $\S = 0.015$ and $\omega_o = 0.6$ rad/sec

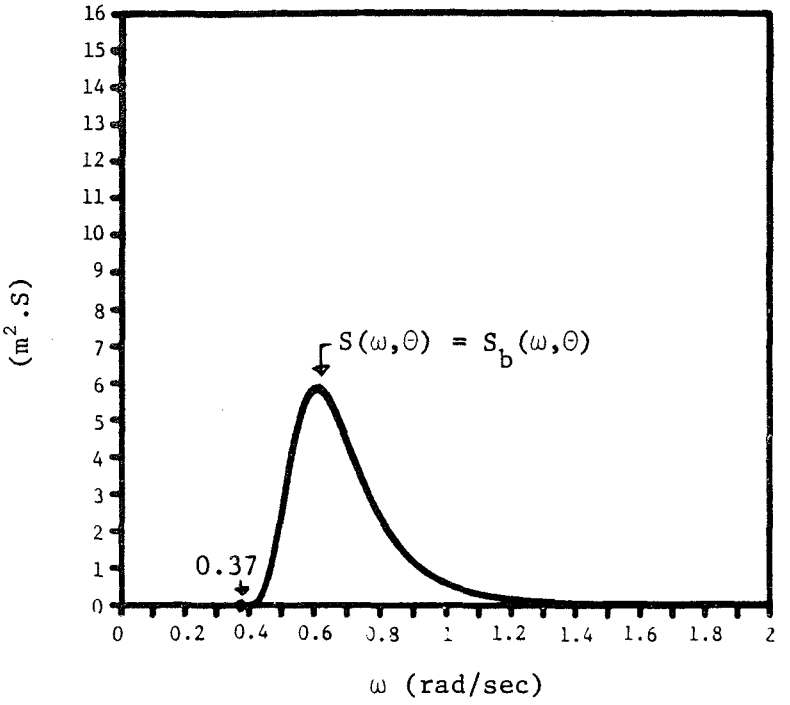

Figure 25. Spectra $S(\omega,\Theta)$ and $S_b(\omega,\Theta)$ of waves at water depth $d = 10^m$ under zero current condition, for $\Theta = 20°$, and $\S = 0.015$ and $\omega_o = 0.6$ rad/sec

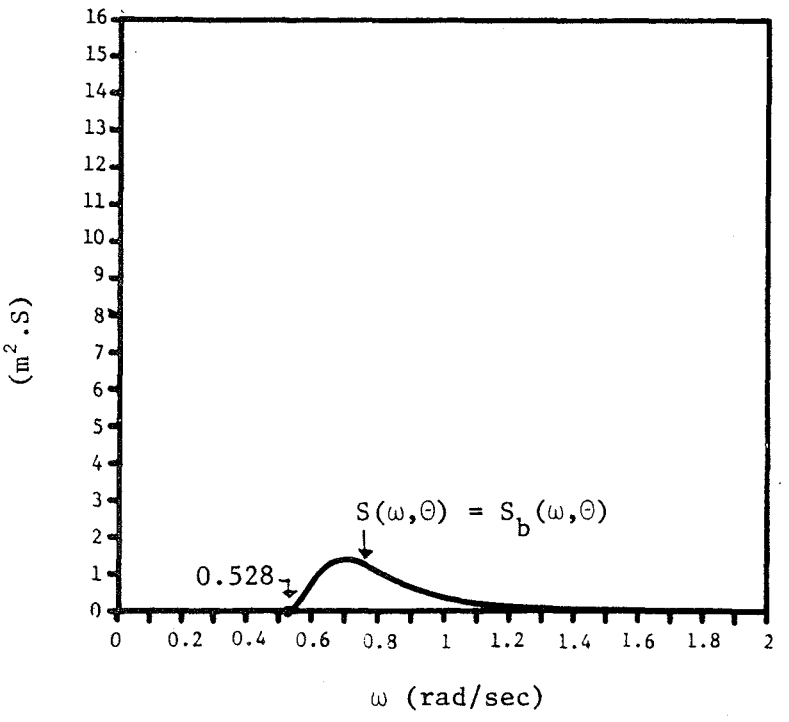

Figure 26. Spectra $S(\omega,\Theta)$ and $S_b(\omega,\Theta)$ of waves at water depth $d = 10^m$ under zero current condition, for $\Theta = 30°$, and $\S = 0.015$ and $\omega_o = 0.6$ rad/sec

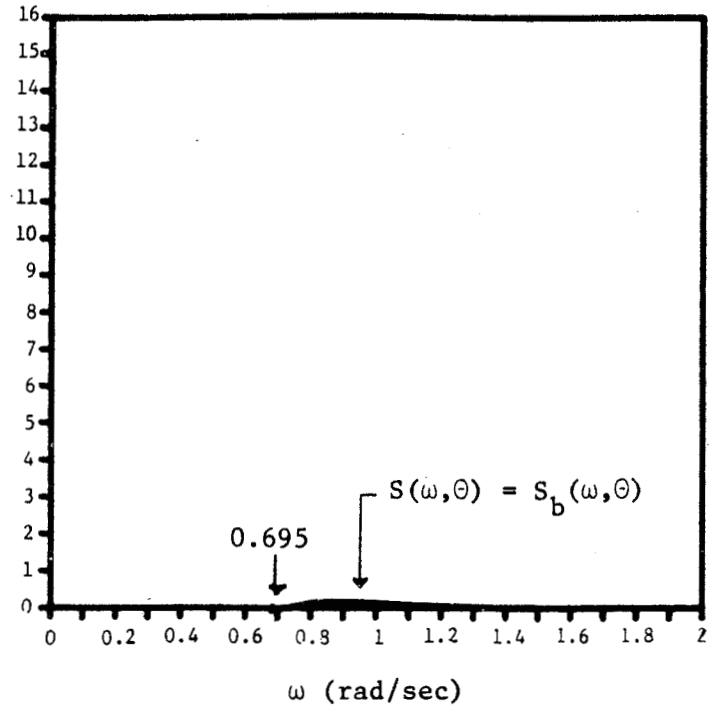

Figure 27. Spectra $S(\omega,\Theta)$ and $S_b(\omega,\Theta)$ of waves at water depth $d = 10^m$ under zero current condition, for $\Theta = 40°$, and $\S = 0.015$ and $\omega_o = 0.6$ rad/sec

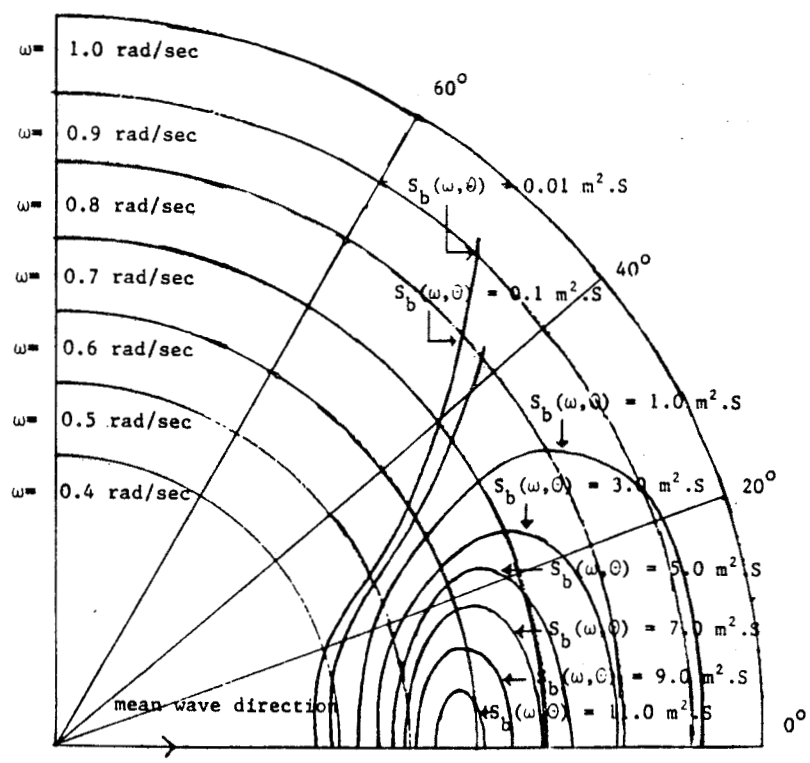

Figure 28. Contour lines of $S_b(\omega,\Theta)$ of waves at water depth $d = 10^m$ under zero current condition, for $\S = 0.015$ and $\omega_o = 0.6$ rad/sec

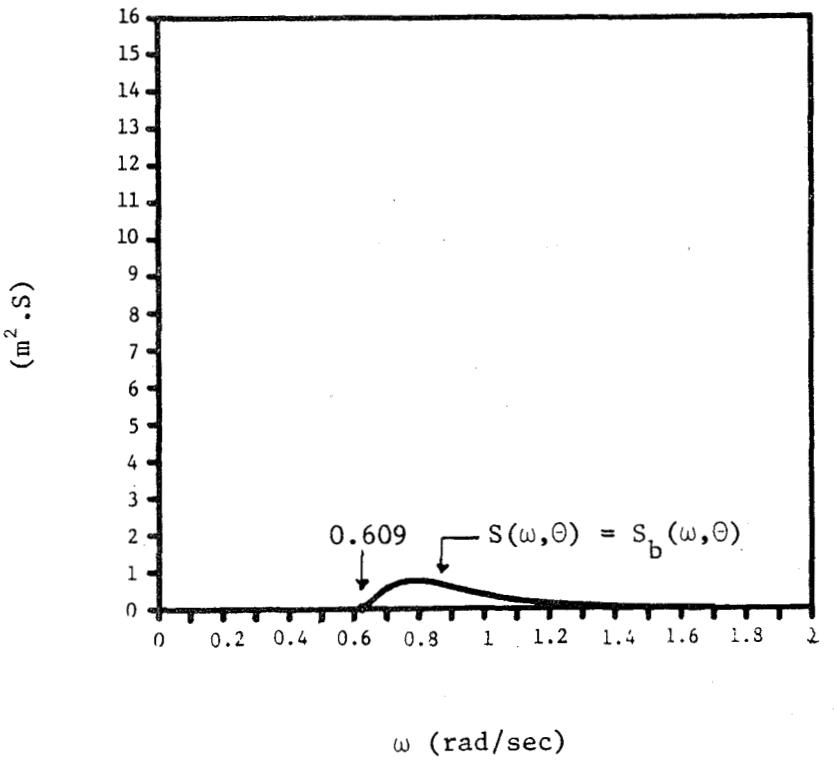

Figure 29. Spectra $S(\omega,\Theta)$ and $S_b(\omega,\Theta)$ of waves at water depth $D = 10^m$ on current with $V = 2^m/_s$, for $\Theta = -30°$, and for $\S = 0.015$ and $\omega_o = 0.6$ rad/sec

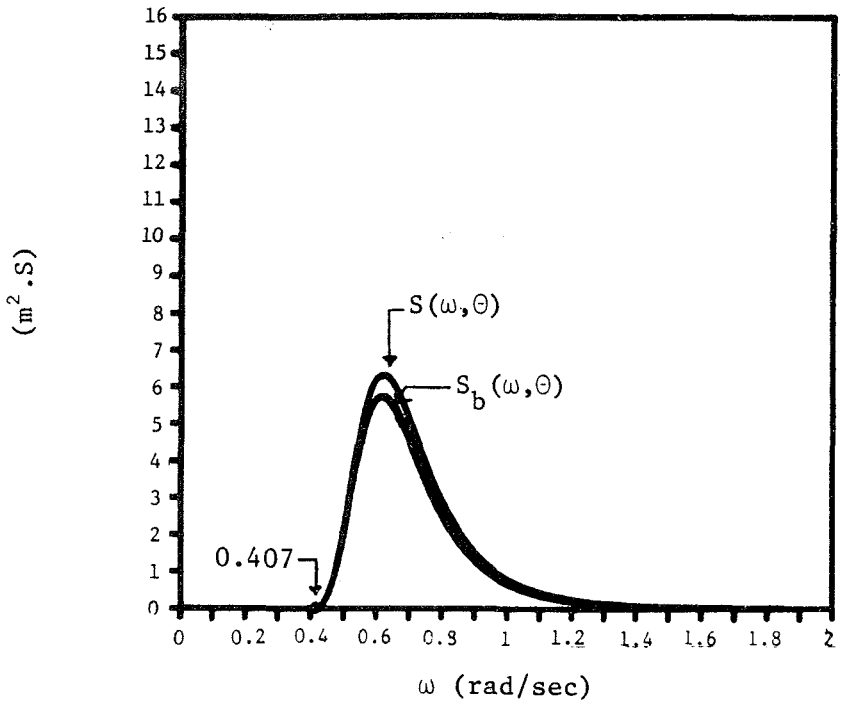

Figure 30. Spectra $S(\omega,\Theta)$ and $S_b(\omega,\Theta)$ of waves at water depth $d = 10^m$ on current with $V = 2^m/_s$, for $\Theta = -20°$, and for $\S = 0.015$ and $\omega_o = 0.6$ rad/sec

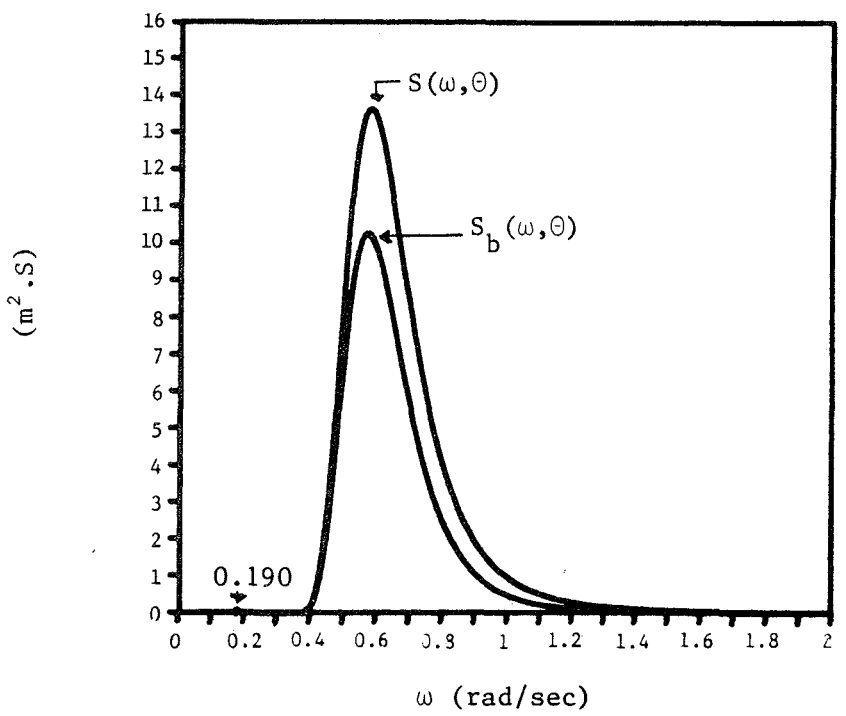

Figure 31. Spectra $S(\omega,\Theta)$ and $S_b(\omega,\Theta)$ of waves at water depth $d = 10^m$ on current with $V = 2^m/_s$, for $\Theta = -10°$, and for $\S = 0.015$ and $\omega_o = 0.6$ rad/sec

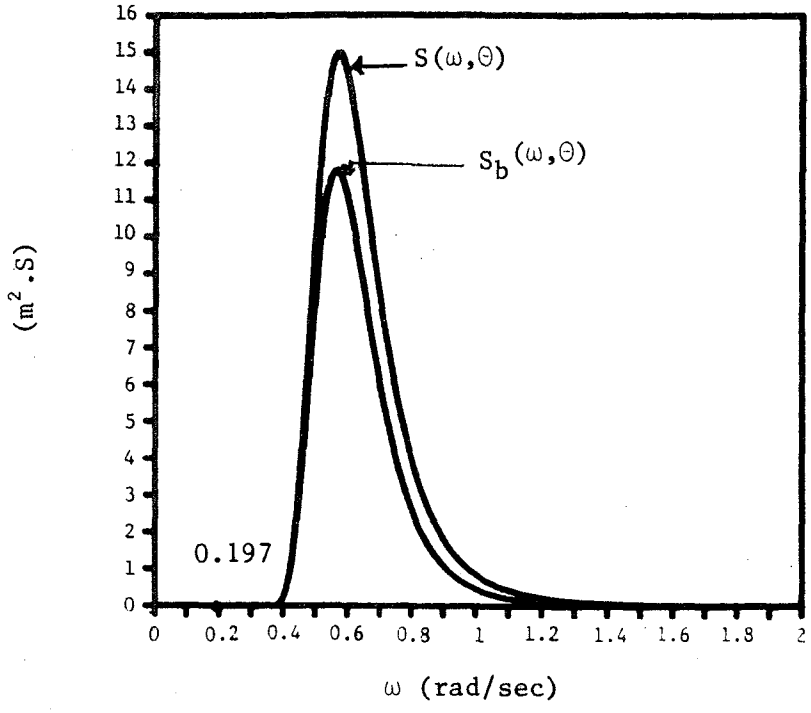

Figure 32. Spectra $S(\omega,\Theta)$ and $S_b(\omega,\Theta)$ of waves at water depth $d = 10^m$ on current with $V = 2^m/_s$, for $\Theta = 0°$, and for $\S = 0.015$ and $\omega_o = 0.6$ rad/sec

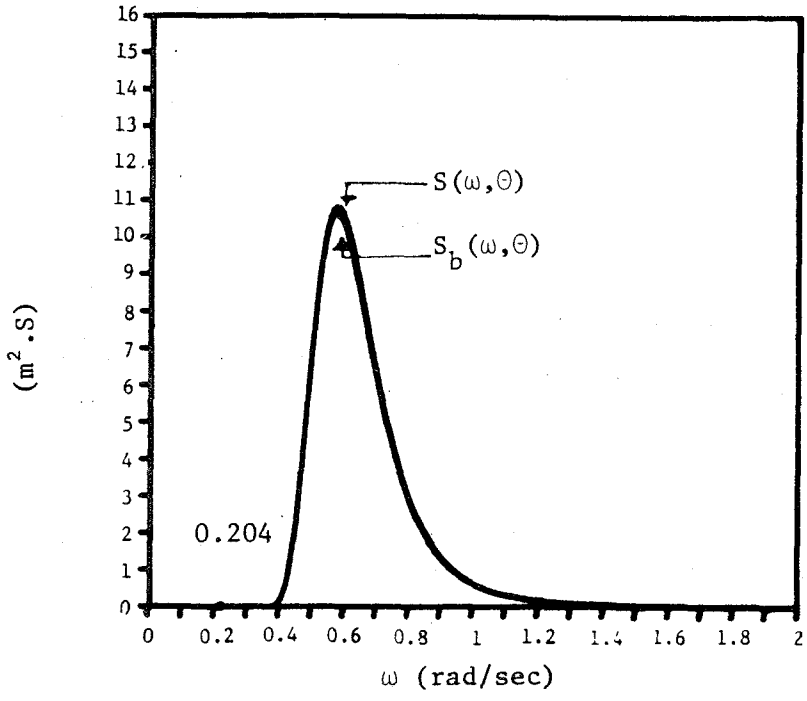

Figure 33. Spectra $S(\omega,\Theta)$ and $S_b(\omega,\Theta)$ of waves at water depth $d = 10^m$ on current with $V = 2^m/_s$, for $\Theta = 10°$, and for $\S = 0.015$ and $\omega_o = 0.6$ rad/sec

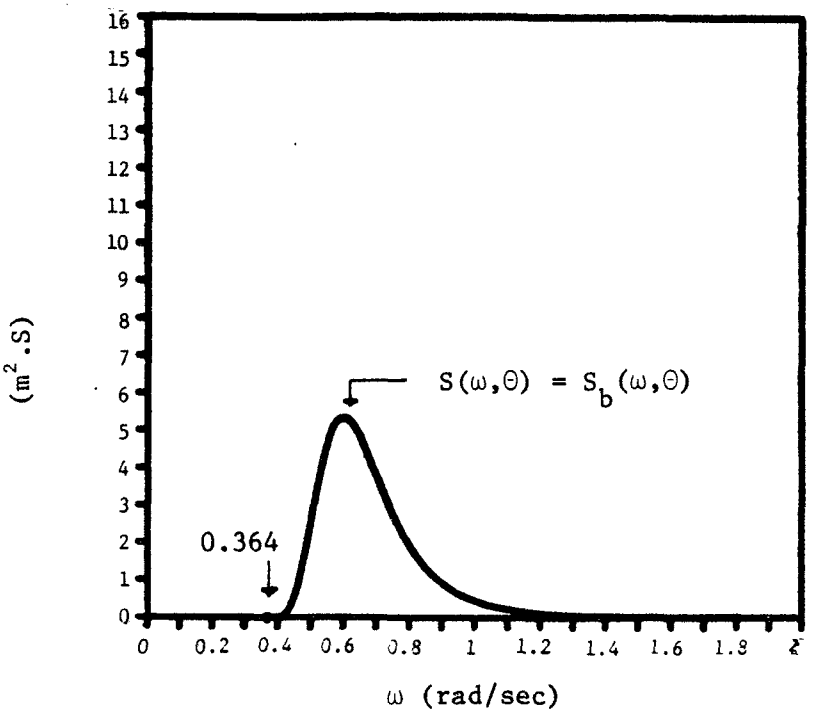

Figure 34. Spectra $S(\omega,\Theta)$ and $S_b(\omega,\Theta)$ of waves at water depth $d = 10^m$ on current with $V = 2^m/_s$, for $\Theta = 20°$, and for $\S = 0.015$ and $\omega_o = 0.6$ rad/sec

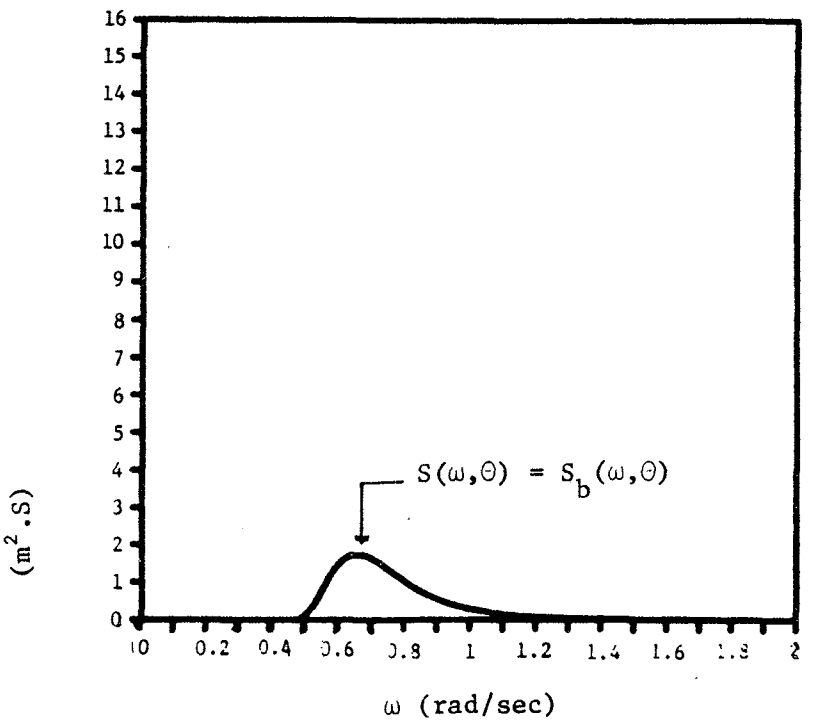

Figure 35. Spectra $S(\omega,\Theta)$ and $S_b(\omega,\Theta)$ for waves at water depth $d = 10^m$ on current with $V = 2^m/_s$, for $\Theta = 30°$, and for $\S = 0.015$ and $\omega_o = 0.6$ rad/sec

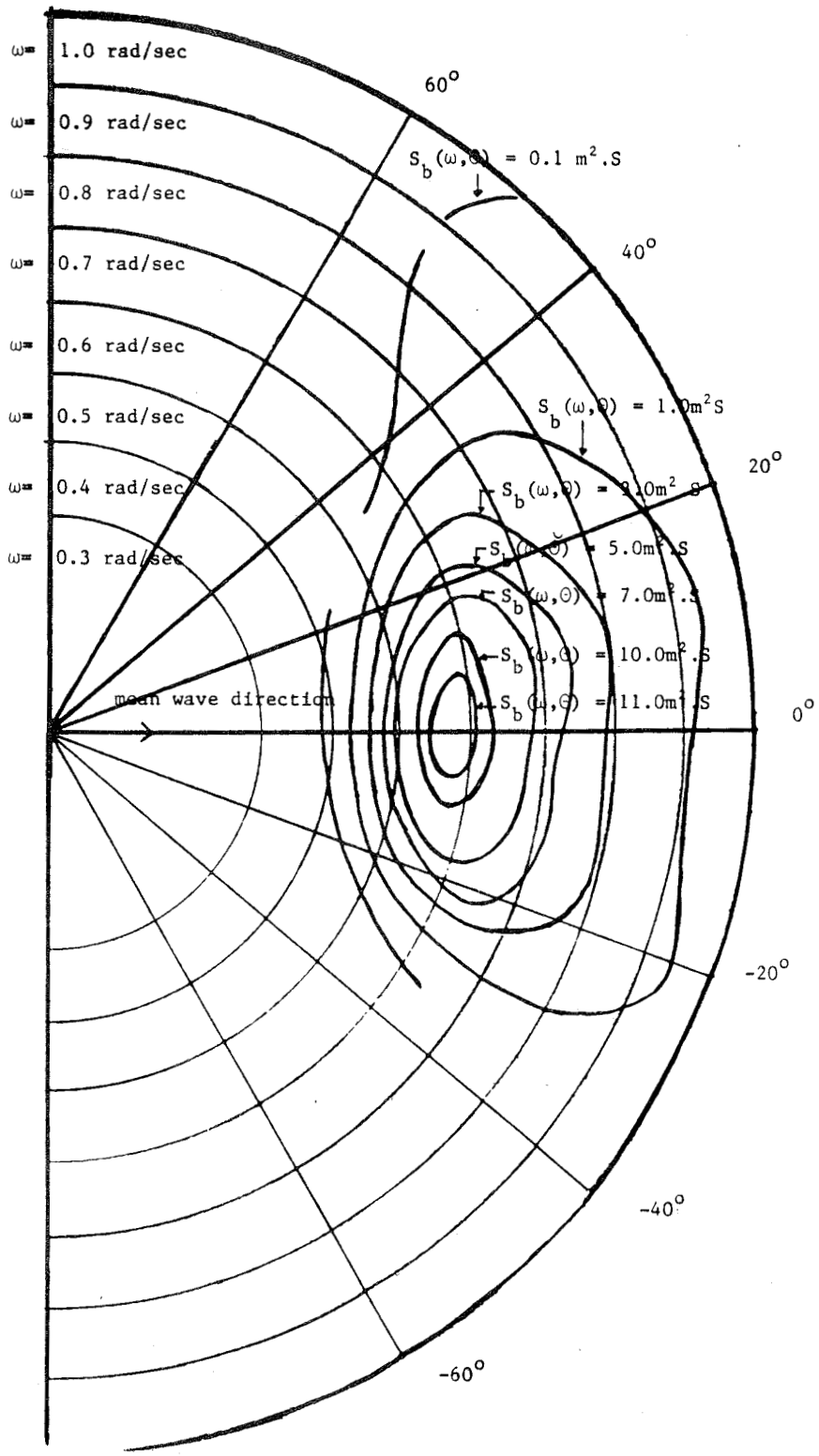

Figure 36. Contour lines of $S_b(\omega,\Theta)$ of waves at water depth $D = 10^m$ on current with $V = 2^m/_s$, for $\Theta = 0.015$ and $\omega_o = 0.6$ rad/sec

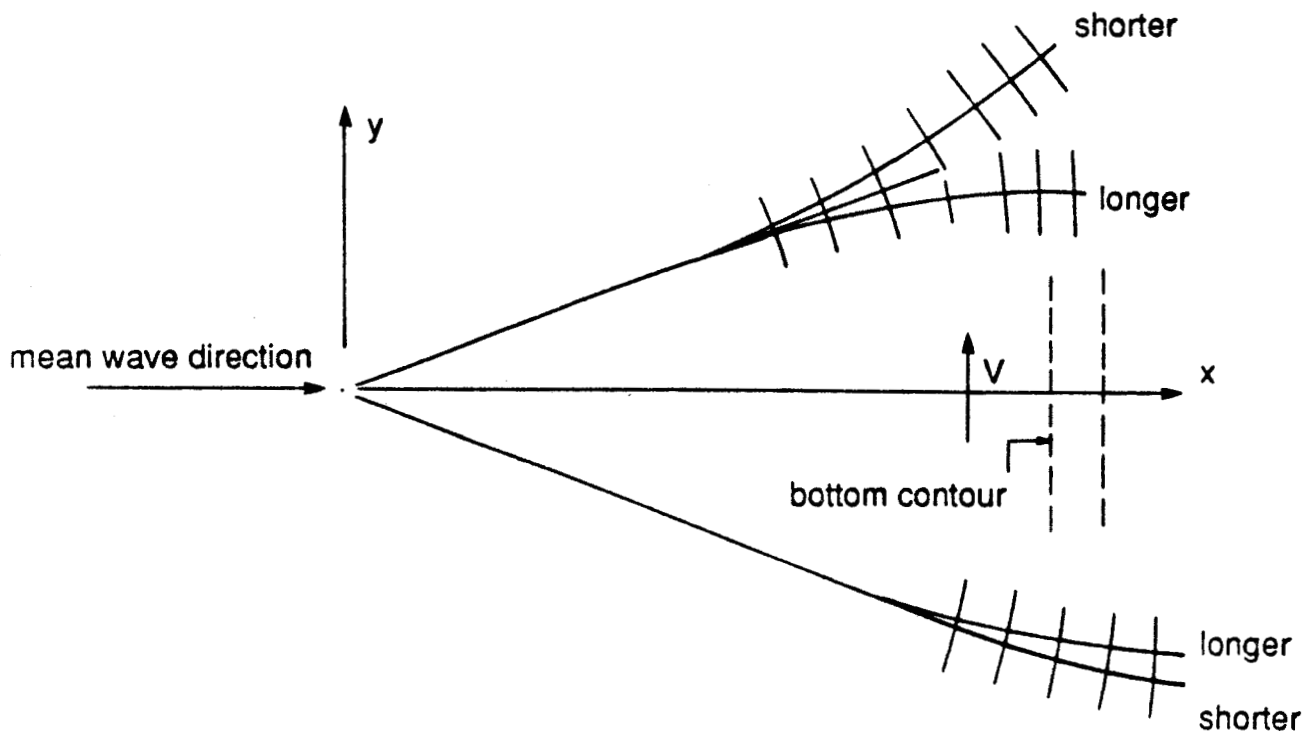

Figure 37. Qualitative behavior of waves on positive shear current over bottom of parallel contours

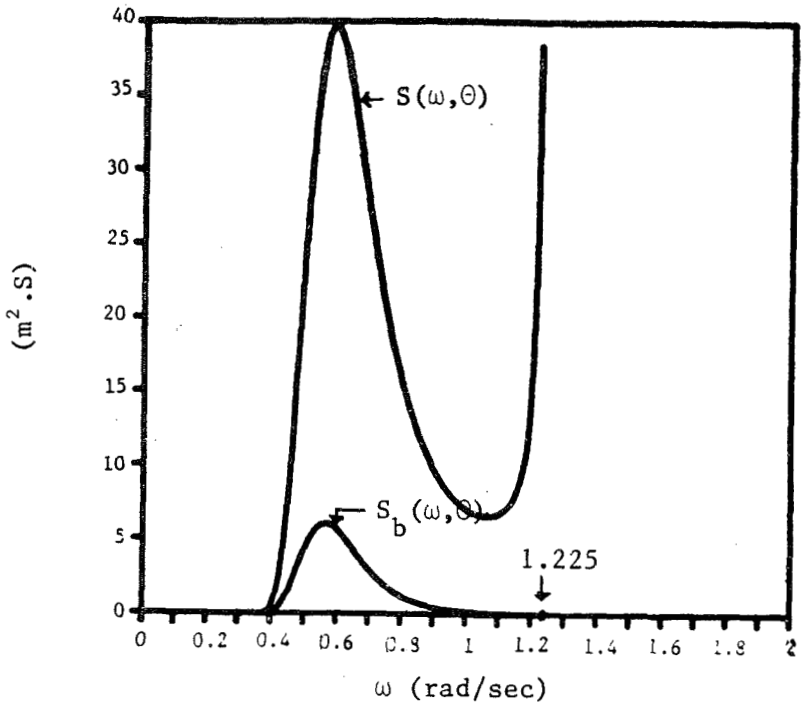

Figure 38. Spectra $S(\omega,\Theta)$ and $S_b(\omega,\Theta)$ of waves at water depth $d = 10^m$ on current with $U = -2^m/_s$, for $\Theta = 0°$, and for $\S = 0.015$ and $\omega_o = 0.6$ rad/sec

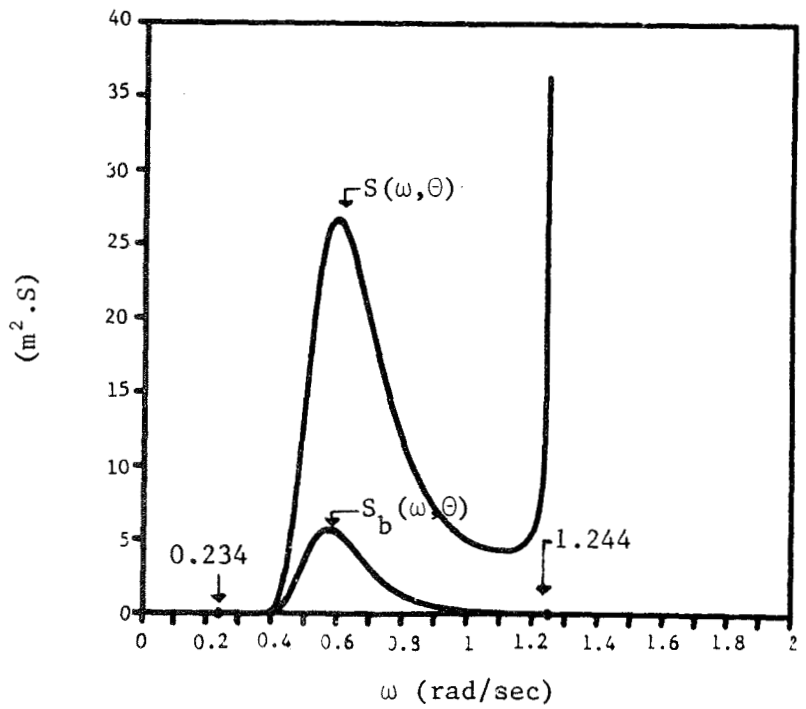

Figure 39. Spectra $S(\omega,\Theta)$ and $S_b(\omega,\Theta)$ of waves at water depth $d = 10^m$ on current with $U = -2^m/_s$, for $\Theta = 10°$, and for $\S = 0.015$ and $\omega_o = 0.6$ rad/sec

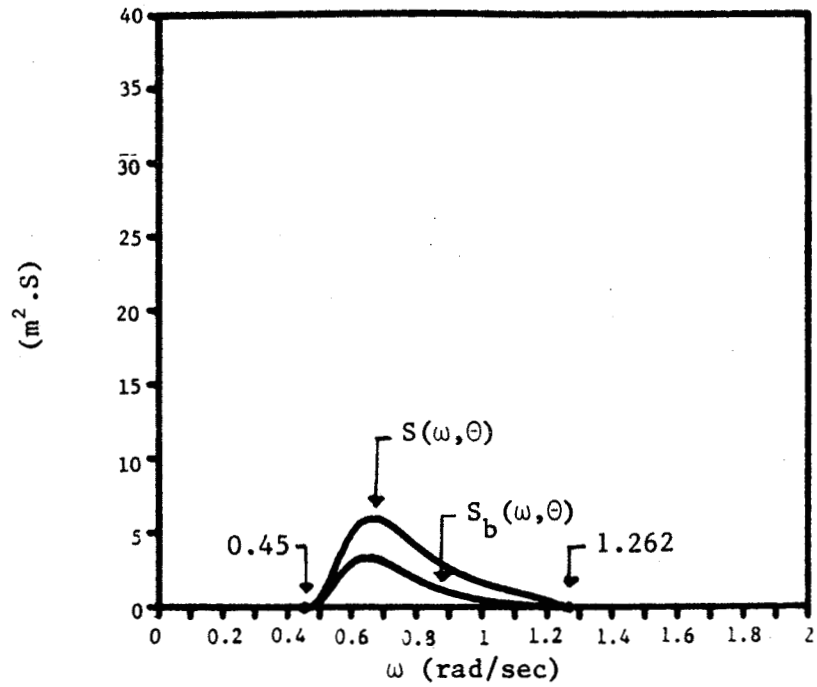

Figure 40. Spectra $S(\omega,\Theta)$ and $S_b(\omega,\Theta)$ of waves at water depth $d = 10^m$ on current with $U = -2^m/_s$, for $\Theta = 20°$, and for $\S = 0.015$ and $\omega_o = 0.6$ rad/sec

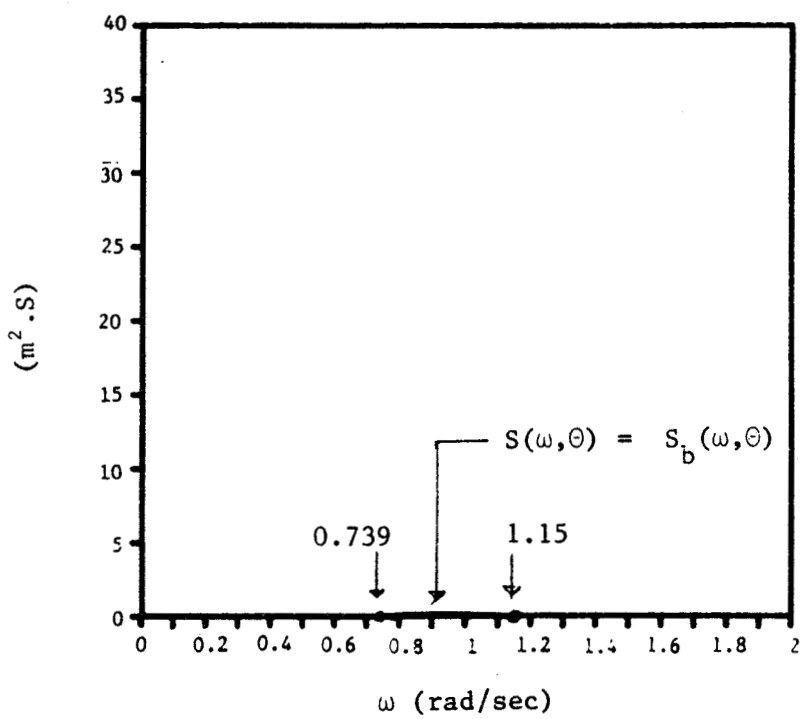

Figure 41. Spectra $S(\omega,\Theta)$ and $S_b(\omega,\Theta)$ of waves at water depth $d = 10^m$ on current with $U = -2^m/_s$, for $\Theta = 30°$, and for $\S = 0.015$ and $\omega_o = 0.6$ rad/sec

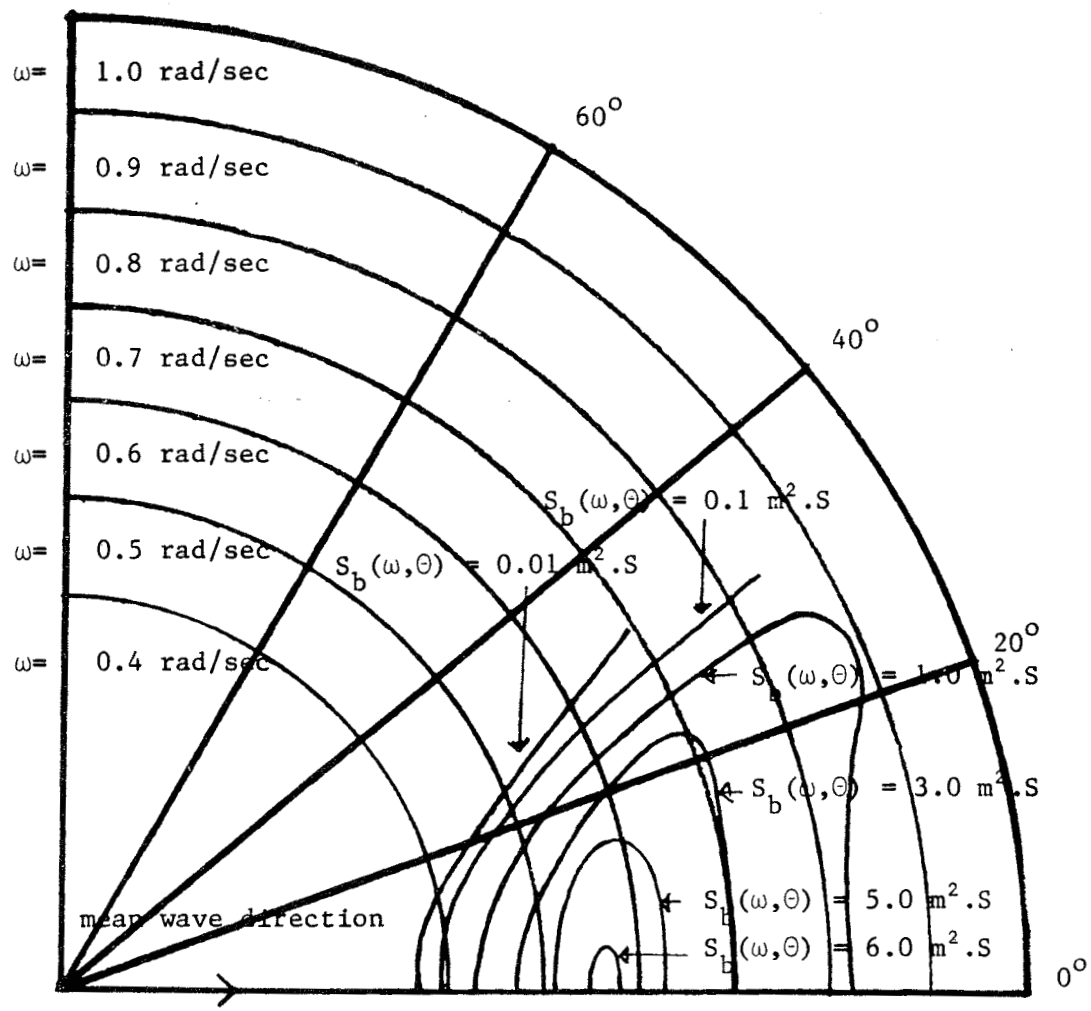

Figure 42. Contour lines of $S_b(\omega,\Theta)$ of waves at water depth $d = 10^m$ on current with $U = -2^m/_s$, for $\S = 0.015$ and $\omega_o = 0.6$ rad/sec

APPENDIX A: NOTATION

A_1, A_2	Quantities defined in Equations 17 and 18, respectively
$(C_g)_\infty, C_{gr}$	Group velocities defined in Equation 24 and 25, respectively
$d(x)$	Water depth
$E[.]$	Expected value of the quantity enclosed in the brackets
$F(\omega)$	Filter function defined in Equation 8
g	Gravitational acceleration
$H(\cdot)$	Heaviside unit step function
K	Coefficient defined in Equation 4
k	Magnitude of wave number vector $\underset{\sim}{k}$
$\underset{\sim}{k}$	Wave number vector
k_∞	Magnitude of wave number in deep water
$\bar{k}_o$	Characteristic wave number in deep water
m	Magnitude of the slope of the Wallops spectrum for deep water waves in the high frequency range on log-log scale given in Equation 38
$\bar{N}$	Quantity defined in Equation 19
n	Quantity defined in Equation 26
$Q(\cdot)$	Probability function defined in Equation 10
$R_b(\tau)$	Autocorrelation function of breaking wave elevation $\zeta_b(t)$
$r, r^{(2)}, r^{(4)}$	Quantities defined in Equations 11, 12, and 13, respectively
$S(\omega)$	Ideal wave spectrum
$S_b(\omega)$	Breaking wave spectrum
$S_\infty(\omega)$	Spectrum of waves in deep water
$S(\omega, \Theta)$	Directional spectrum of ideal waves in absolute frame of reference
$S_b(\omega, \Theta)$	Directional spectrum of breaking waves in absolute frame of reference

$\overline{S}(\omega_r,\Theta)$	Directional spectrum of ideal waves in relative frame of reference
$\overline{S}_b(\omega_r,\Theta)$	Directional spectrum of breaking waves in relative frame of reference
$S_\infty(\omega,\Theta_\infty)$	Directional Spectrum in quiescent deep water
t	Time
t_1,t_2	Time instants $t + \tau$ and t, respectively
$U(x)$	Speed of current of the upwelling type in the x-direction
$\underset{\sim}{U}_H$, U_H	Horizontal current velocity vector and its magnitude, respectively
$V(x)$	Speed of shear current in the y-direction
x,y	Horizontal coordinates defined in Figure 1
$Z(\cdot)$	Probability function defined in Equation 9
α	Coefficient defined in Equation 40
β	Wave Breaking parameter defined in Equation 14
$\Gamma(\cdot)$	The gamma function
ε	Spectral bandwidth parameter defined in Equation 15
$\zeta(t)$, $\zeta_b(t)$	Elevations of ideal and breaking waves, respectively
η	Dummy variable
Θ,θ_∞	Angles of wave at locale under consideration and in deep water, respectively
λ_o	Characteristic wave length
ξ	Dummy variable
τ	Time lag
$\Phi(\cdot)$	Directional energy spreading function defined in Equation 36
ω	Wave frequency
ω_r	Wave frequency in relative frame of reference
$\overline{\omega}$	Characteristic wave frequency defined in Equation 6

ω_o	Parameter of Wallops Spectrum
ω_1	Quantity defined in Equation 16

<u>Subscripts</u>

1,2	Quantities evaluated at time instants t_1, and t_2, respectively
∞	Quantities evaluated in deep water under zero current condition

<u>Symbols</u>

.	Differentiation with respect to time
§	Significant wave slope defined in Equation 39